Probing single-particle structures via <u>proton</u>-induced knockout reactions

Kazuyuki Ogata

Research Center for Nuclear Physics (RCNP), Osaka University

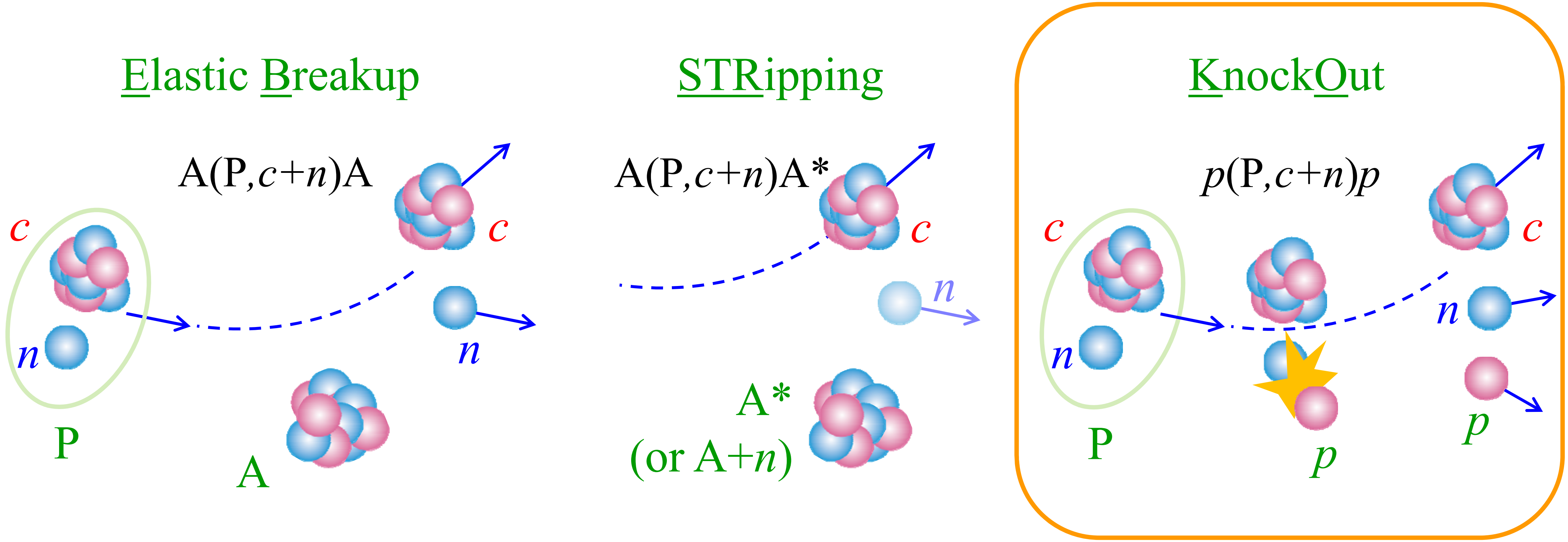

Contents

- Classification of reaction processes and reaction models
  - (*p*,*pN*) for studying s.p. properties of nuclei in the ground state
  - Distorted Wave Impulse Approximation (DWIA)

- Mechanism of the asymmetry in the parallel momentum distribution (PMD)
  - The phase volume effect on the high-mom. side
  - Distortion (momentum shift) effect on the low-mom. side

- Many physics cases related to (*p*,*pN*)

Spectroscopy with breakup reactions

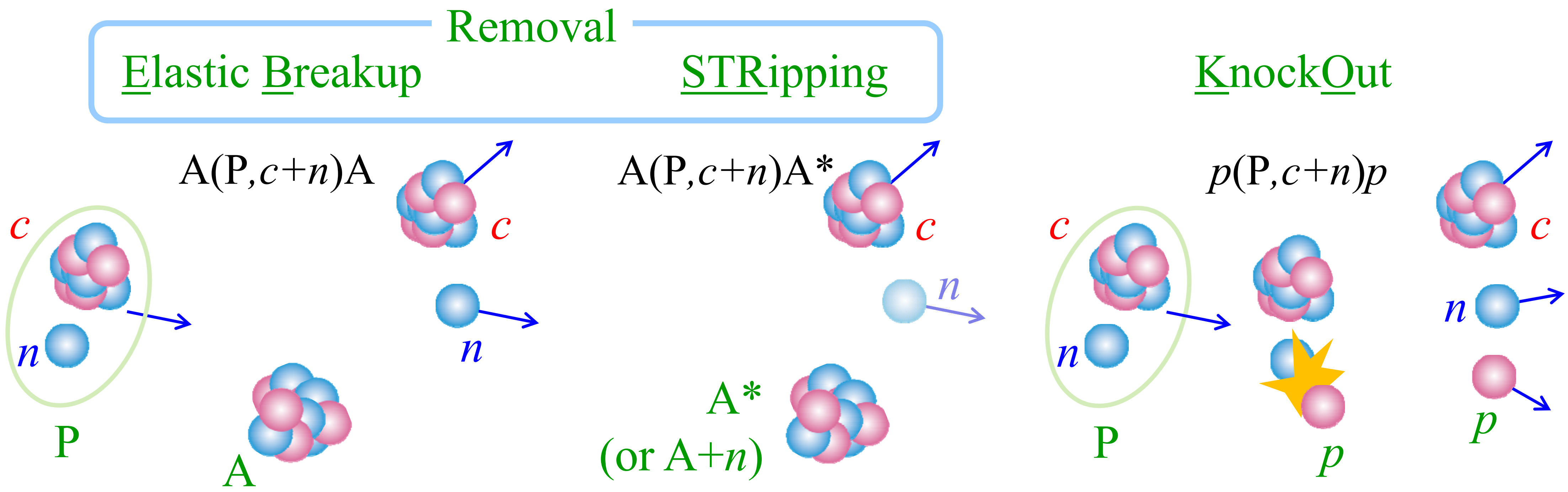

- A is not excited.
- Small energy-momentum transfer (ω-*q*)
- CDCC, DEA, Faddeev-AGS etc. are available.

- A is excited.
- Contribution from *Q*-space.
- Formulation is difficult (Glauber, ERT).

- A kind of EB
- Large ω-*q*
- DWIA(QFS picture)

Missing Correlations (the Gade plot)

A. Gade *et al*., PRC**77**, 044306 (2008) [updated in Tostevin and Gade, PRC**90**, 057602 (2014)].

Reduction of spectroscopic strength: Weakly-bound and strongly-bound single-particle states studied using one-nucleon knockout reactions

Understanding level

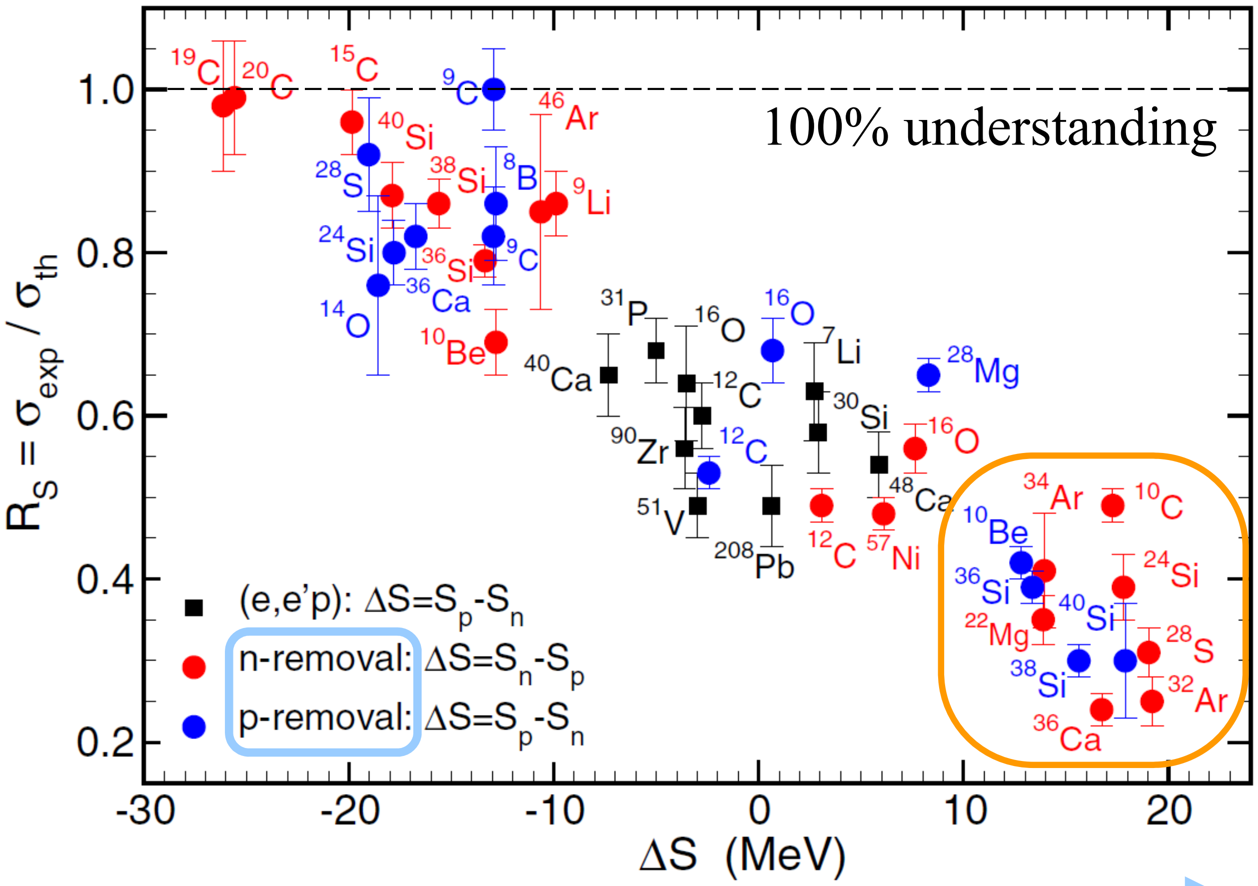

60–80% missing correlations!

Separation energy of struck nucleon

Some counterarguments

J. Lee, private communication*

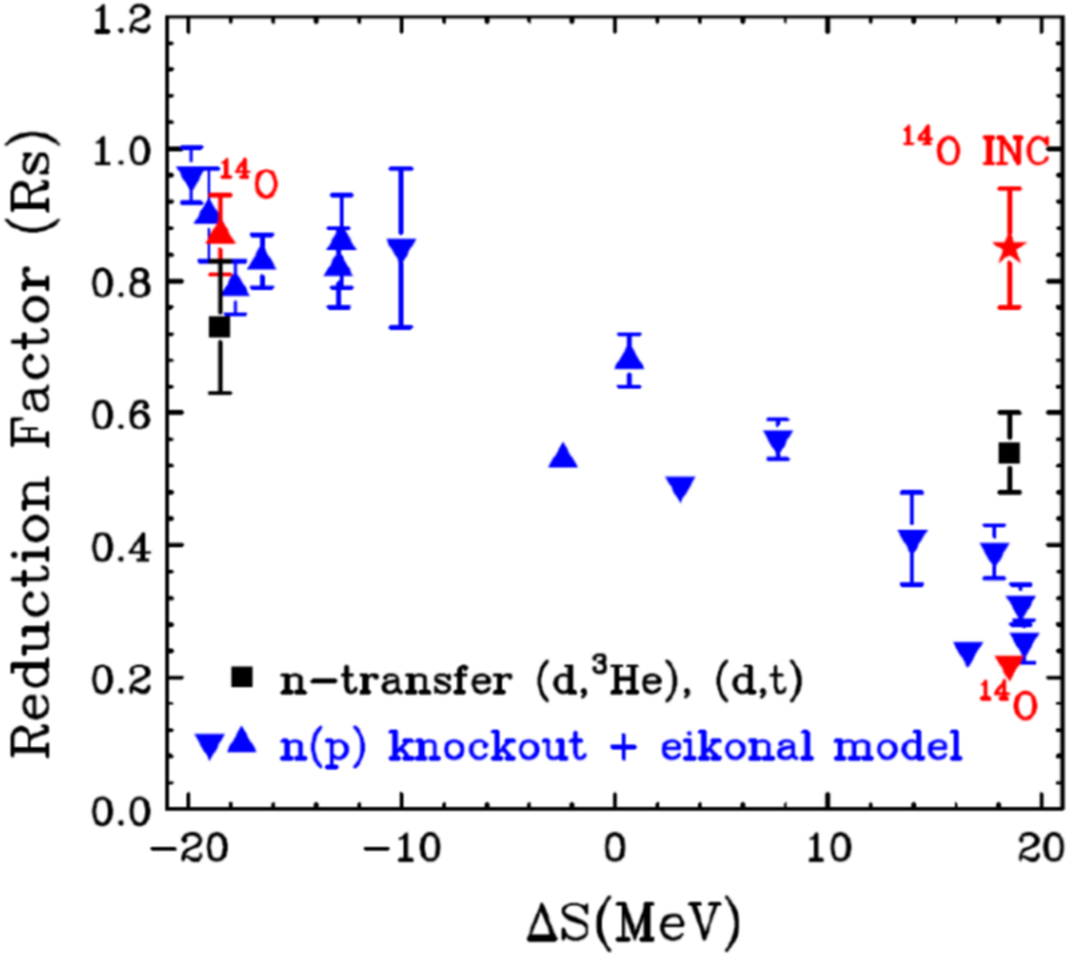

F. Flavigny *et al.*, PRL**110**, 122503 (2013).

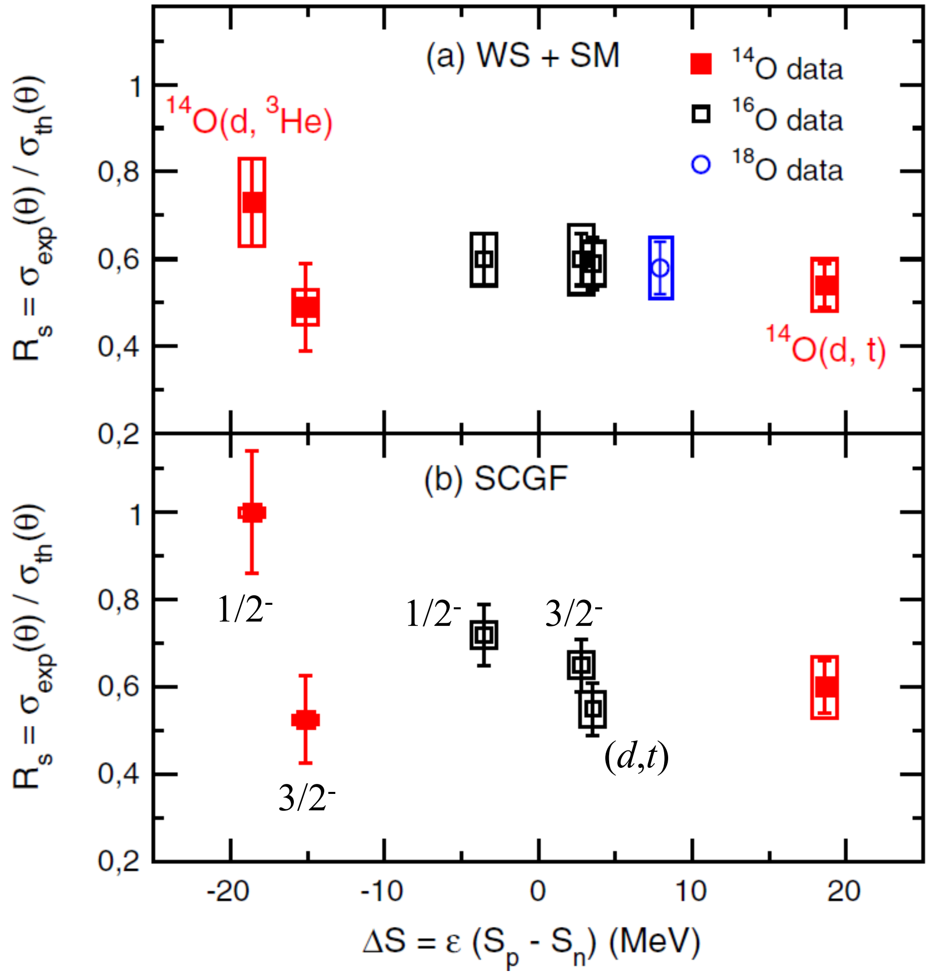

*A compilation of A. Gade *et al.*, PRC**77**, 044306 (2008),
F. Flavigny *et al.*, PRL**108**, 252501 (2012), and
F. Flavigny *et al.*, PRL**110**, 122503 (2013).

Asymmetry of $P_{//}$

F. Flavigny *et al.*, PRL **108**, 252501 (2012).

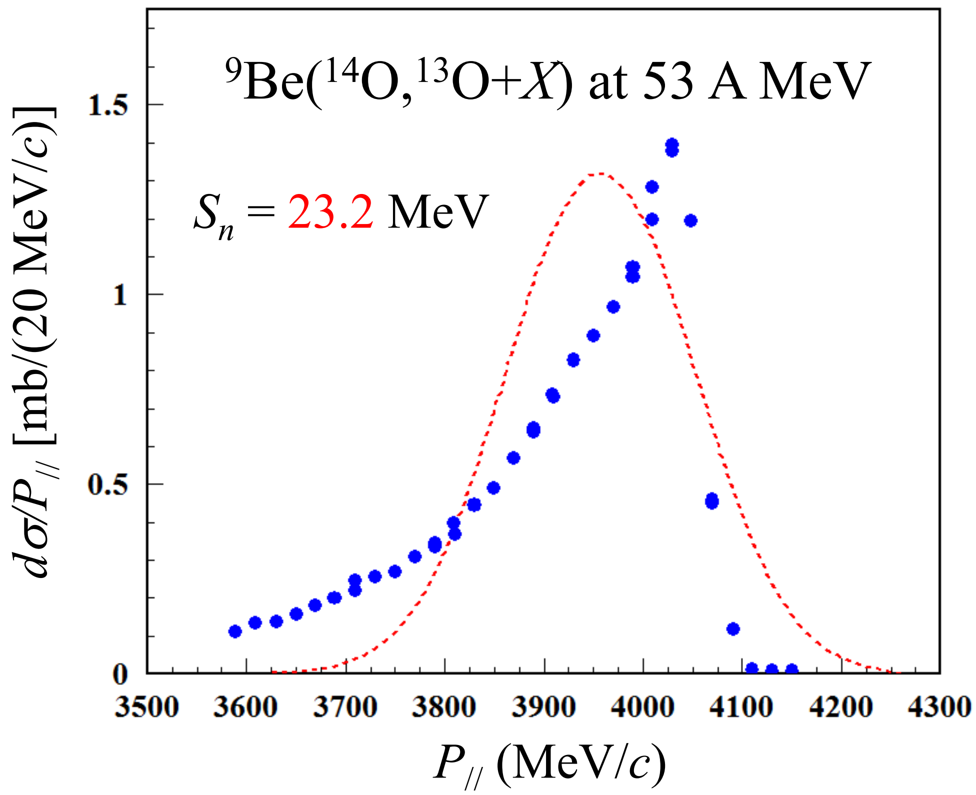

^{12}C(^{31}Ne,^{30}Ne+*X*) at 230 A MeV

T. Nakamura *et al.*, PRL**112**, 142501 (2014).

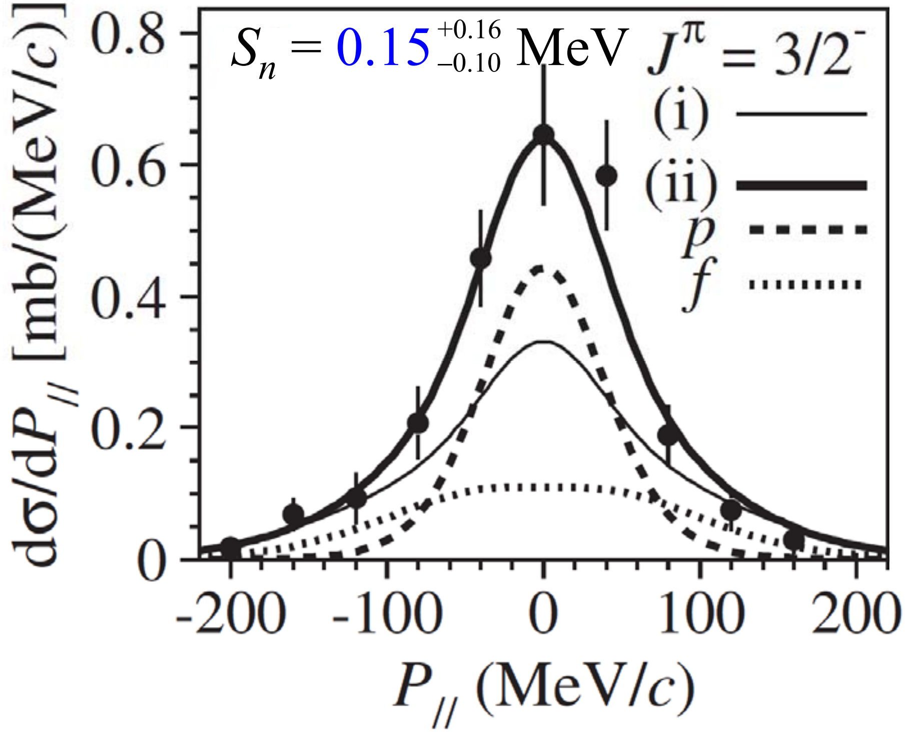

- ✓ The Glauber model is usually adopted that gives inevitably a symmetric $P_{//}$ because of the <u>AD</u>iabatic (sudden) approximation.
- ✓ For non weak-binding nuclei, $P_{//}$ is asymmetric, which is not understood well.

Our strategy

- We do not have a non-adiabatic framework applicable to stripping processes.
  → We cannot discuss the Gade plot directly.
  cf. Transfer to continuum model by Bonaccorso and Brink, PRC **38**, 1776 (1988).
  Revival of the Ichimura-Austern-Vincent model by J. Lei and Moro, PRC **92**, 044616 (2015).
- We focus on the EB and KO processes and aim at finding the mechanism that generates the asymmetry in the PMD, with clarifying why the Glauber model cannot explain it (for EB).
  → If the mechanism exists also in stripping processes, we may regard it as a possible source of the strong quenching of the reduction factor.
- We will use DWIA, which is “equivalent” (and can be superior) to CDCC.

MD of EB in CDCC (or DWIA)

Y. Iseri, Yahiro, Kamimura, PTP Suppl **89**, 84 (1986); G. G. Ohlsen, NIM**37**, 240 (1965).

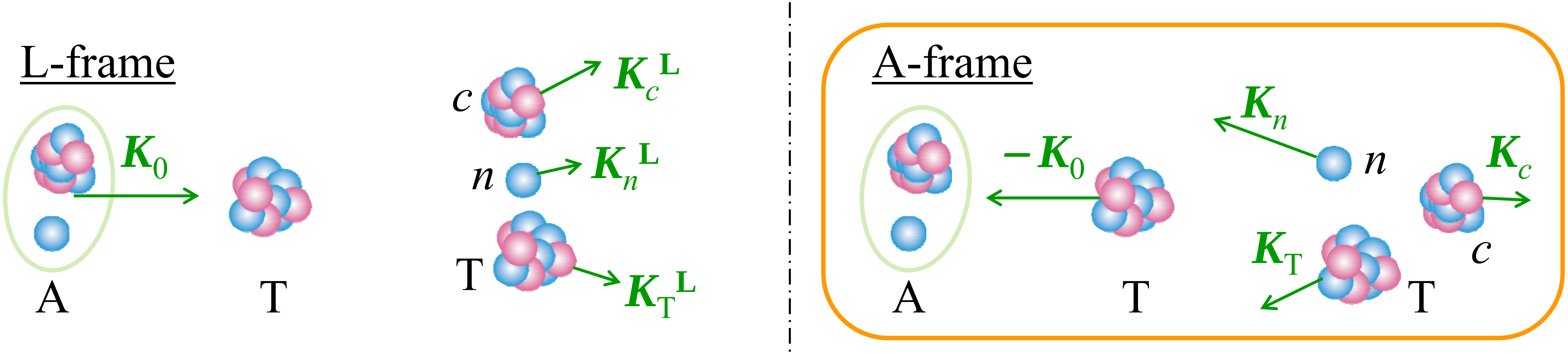

$$\frac{d^3\sigma}{d\boldsymbol{K}_c d\hat{\boldsymbol{K}}_n} = C_0 \rho\left(\boldsymbol{K}_c, \hat{\boldsymbol{K}}_n\right) \left|T_{\beta\alpha}^{\mathrm{CDCC}}\right|^2,$$

$$\rho\left(\boldsymbol{K}_c, \hat{\boldsymbol{K}}_n\right) \equiv \int d\boldsymbol{K}_T K_n^2 dK_n \delta\left(\boldsymbol{K}_\beta - \boldsymbol{K}_\alpha\right) \delta\left(E_\beta - E_\alpha\right).$$

- The Phase Volume guarantees the energy-momentum conservation.

$$\frac{d^3\sigma}{d\boldsymbol{K}_c} = C_0 \int d\hat{\boldsymbol{K}}_n \, \rho\left(\boldsymbol{K}_c, \hat{\boldsymbol{K}}_n\right) \left|T_{\beta\alpha}^{\mathrm{CDCC}}\right|^2.$$

MD of EB in the Glauber model

K. Hencken, Bertsch, and Esbensen, PRC**54**, 3043 (1996).

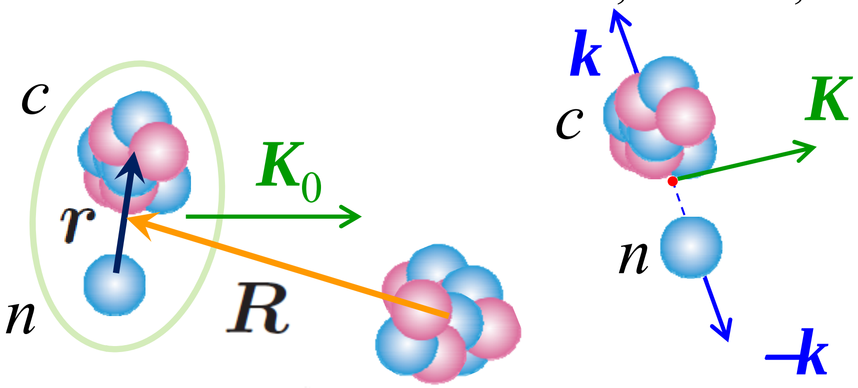

$$\boldsymbol{K} \approx \boldsymbol{K}_0 + K_\perp \boldsymbol{e}_\perp$$

(AD + forward scattering approximation)

$$\frac{d\sigma_{\rm diff}}{(d^2\vec{K}_\perp d^3\vec{k})} = \frac{1}{(2\pi)^5}\frac{1}{2L_0+1}\sum_{M_0}\left|\int d^3\vec{r}\,d^2\vec{R}_\perp e^{-i\vec{K}_\perp\cdot\vec{R}_\perp}\phi^*_{\vec{k}}(\vec{r})S_cS_n\phi_{0,M_0}(\vec{r})\right|^2.$$

- Taking a Jacobi representation results in the simplest form of the PV.
- small ω-q is assumed, with neglecting the E-conservation.

Integration over $\boldsymbol{K}_\perp$ in the whole region

$$\frac{d\sigma_{\rm diff}}{d^3\vec{k}} = \frac{1}{(2\pi)^3}\frac{1}{2L_0+1}\sum_{M_0}\int d^2\vec{R}_\perp\left|\int d^3\vec{r}\,\phi^*_{\vec{k}}(\vec{r})S_cS_n\phi_{0,M_0}(\vec{r})\right|^2.$$

- MD in the A-frame if the mom. of the c-n c.m. is 0.

Preceding discussion on the EB-PMD

J. A. Tostevin *et al*., PRC**66**, 024607 (2002).

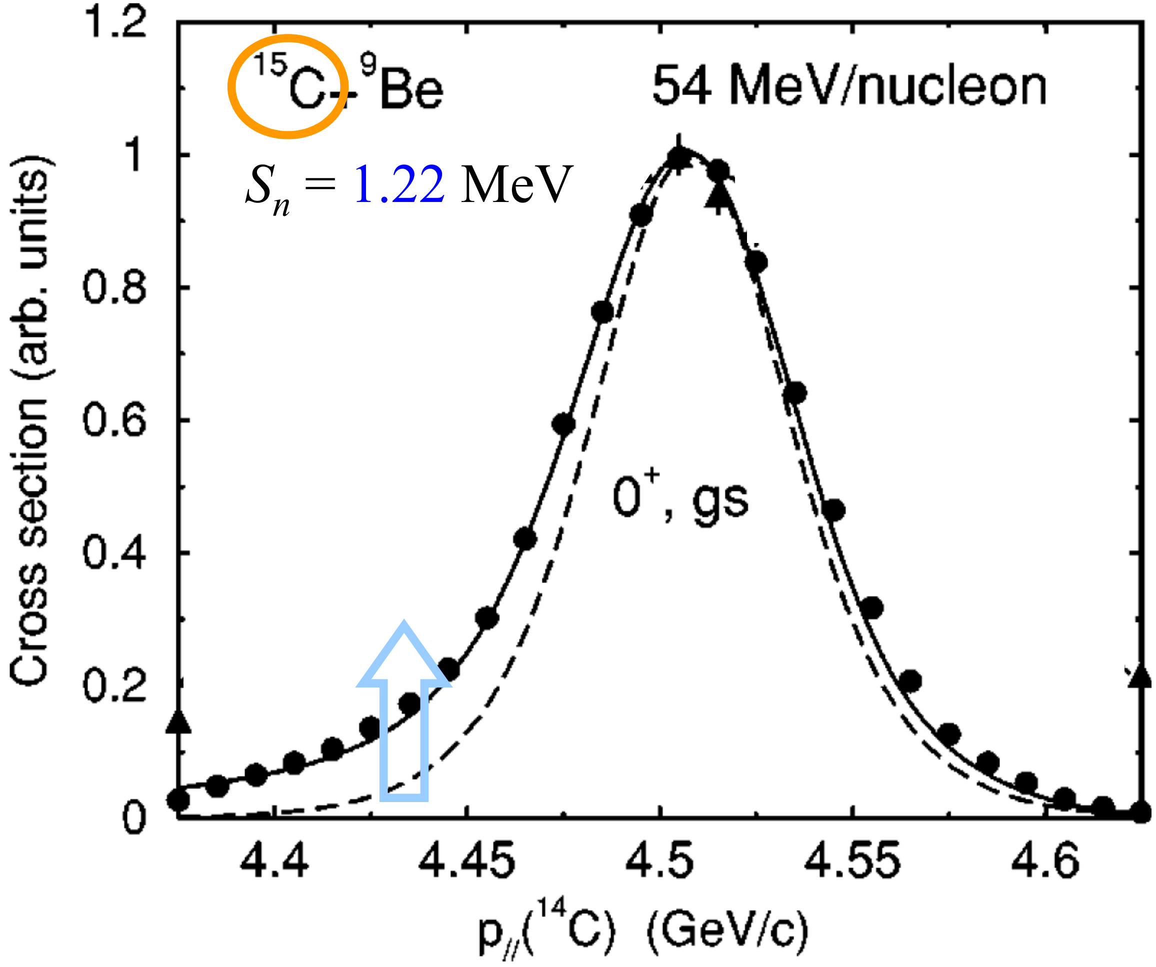

CDCC (EB)+ Glauber (STR)

Glauber (EB&STR)

- The importance of "the accurate three-body dynamics" was claimed.
- The low-mom. tail is often regarded as higher order effects.

Knockout of a tightly bound nucleon

- large ω-q
  - The AD approximation becomes questionable, hence the Glauber model.
  - Higher values of the *c*-*n* breakup energy (and the angular momentum *l*) become necessary.
    → A huge model space is required in CDCC.

- Weak coupling to the breakup channels
  - DWIA is expected to work well.
  - We will focus on reactions with a proton target because of:
    - no contribution of the stripping process
    - observation of the nuclear interior part
    - intuitive picture of the reaction process (DWIA)
  → (p,2p), (p,pn) processes in inverse kinematics

The probed region

M. Yahiro, O, Minomo, PTP **126**, 127 (2011).

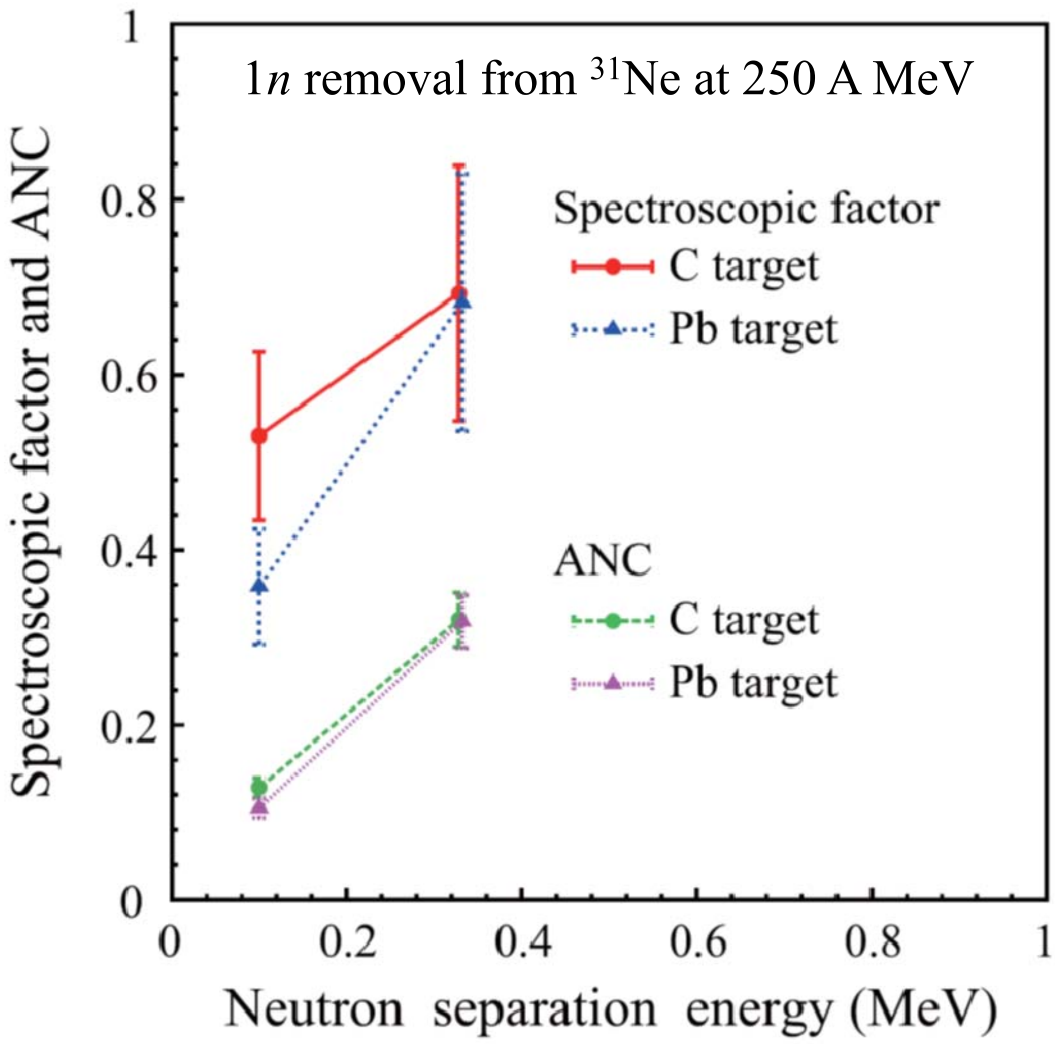

T. Aumann, Bertulani, Ryckebusch, PRC **88**, 064610 (2013).

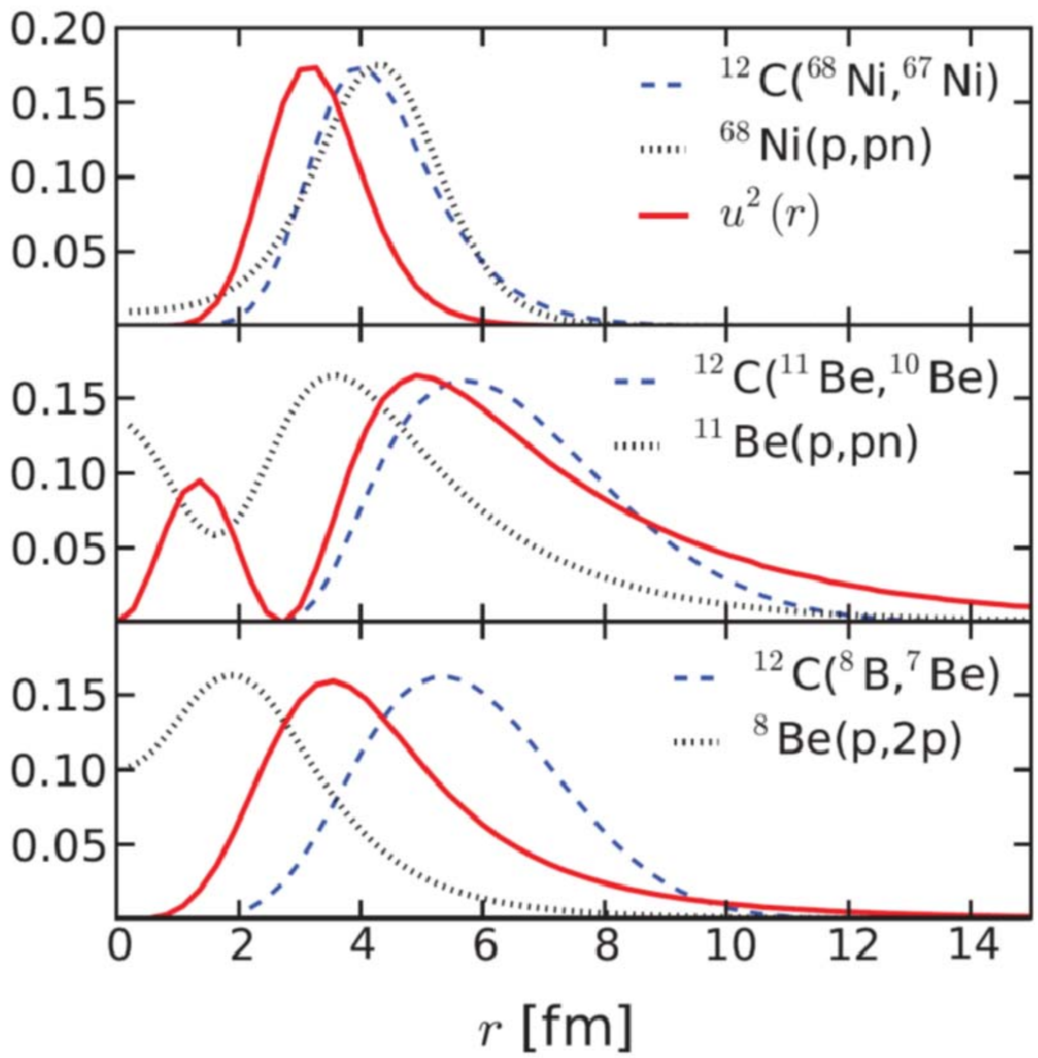

CDCC and DWIA

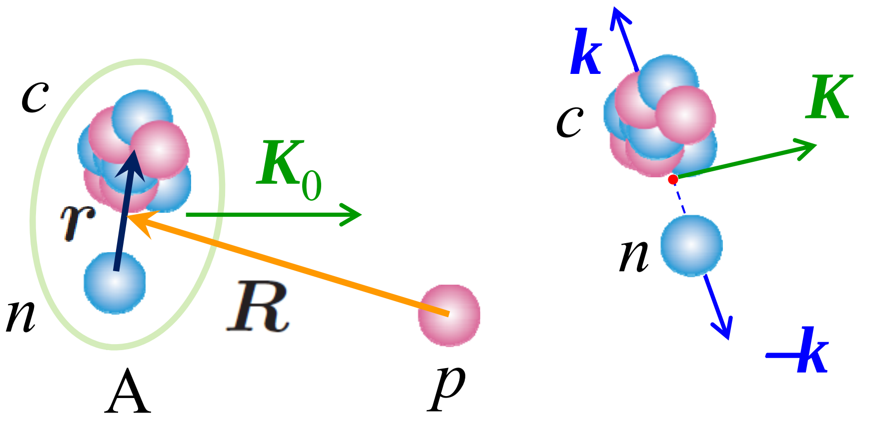

$$T_{\mathrm{CDCC}} = \left\langle \varphi^{(-)}_{nc,\boldsymbol{k}}(\boldsymbol{r})\, e^{i\boldsymbol{K}\cdot\boldsymbol{R}} \middle| v_{pn} + U_{pc} \middle| \sum_i \varphi_i(\boldsymbol{r})\, \chi^{(+)}_i(\boldsymbol{R}) \right\rangle$$

1. Weak coupling to the BU channels

$$\approx \left\langle \varphi^{(-)}_{nc,\boldsymbol{k}}(\boldsymbol{r})\, e^{i\boldsymbol{K}\cdot\boldsymbol{R}} \middle| v_{pn} + U_{pc} \middle| \varphi_0(\boldsymbol{r})\, \underline{\chi^{(+)}_{\mathrm{DW}}}(\boldsymbol{R}) \right\rangle$$

2. Only v_{pn} breaks up A.

p-A elastic wave function

$$\approx \left\langle \underline{\chi^{(-)}_{nc,\boldsymbol{k}}}(\boldsymbol{r})\, \chi^{(-)}_{pc,\boldsymbol{K}}(\boldsymbol{R}) \middle| v_{pn} \middle| \varphi_0(\boldsymbol{r})\, \chi^{(+)}_{\mathrm{DW}}(\boldsymbol{R}) \right\rangle = T_{\mathrm{DWIA}}$$

n-c DW (w/ *E*-dep. complex pot. and/or large *l*)

The Continuum-Discretized Coupled-Channels method: CDCC (conventional CDCC)

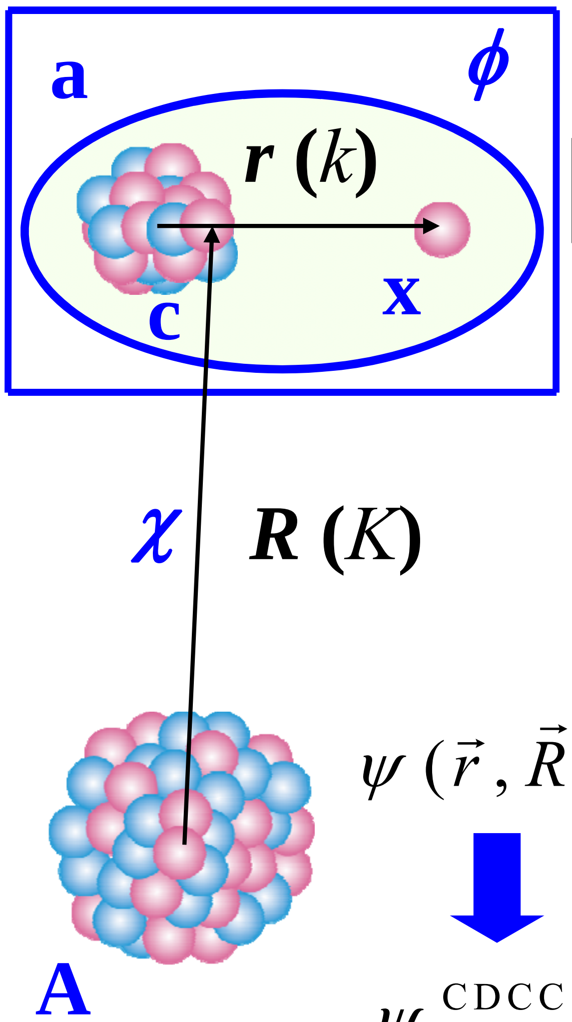

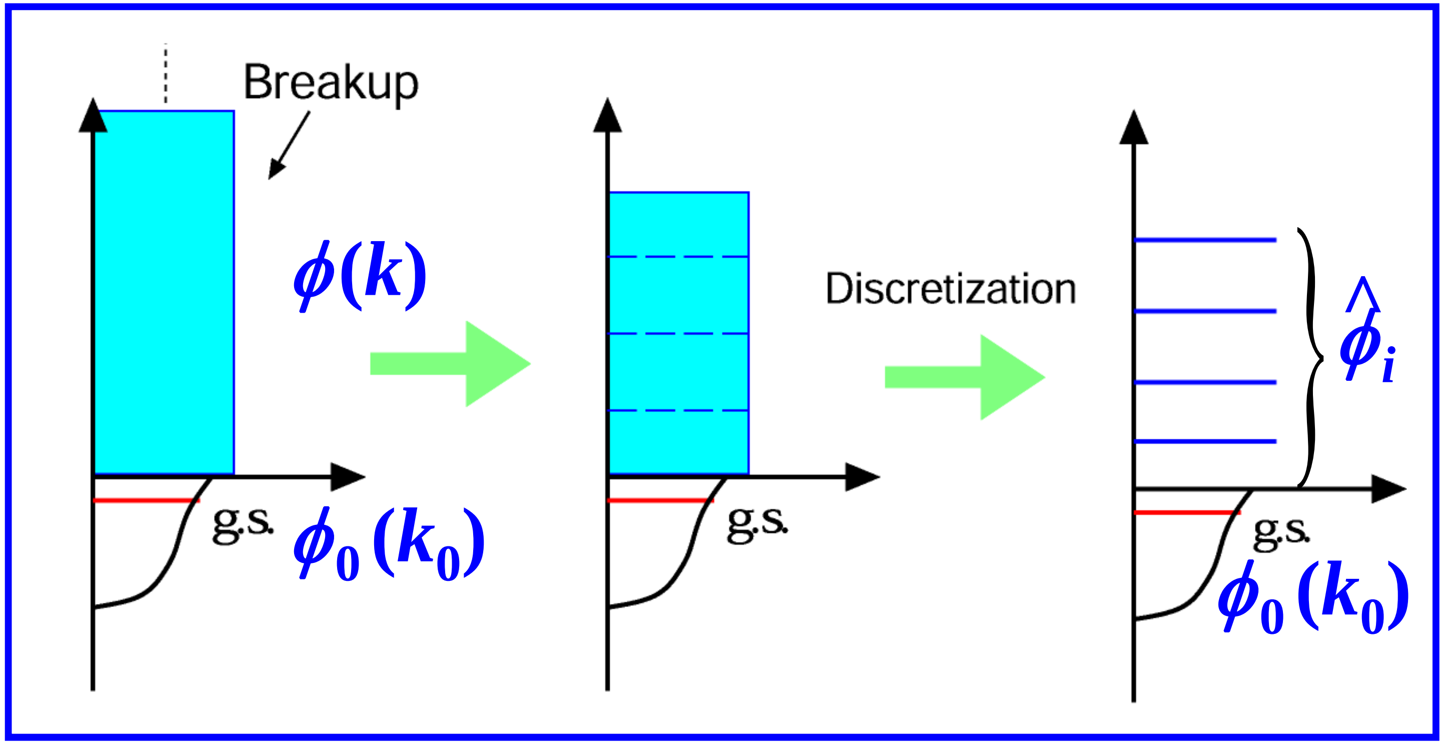

$$\psi(\vec{r},\vec{R}) \cong \phi_0(k_0,\vec{r})\chi_0(K_0,\vec{R}) + \sum_{i=1}^{i_{\max}} \hat{\chi}(\hat{K}_i,\vec{R})\int_{k_{i-1}}^{k_i}\phi(k,\vec{r})dk$$

Truncation and Discretization

$$\psi^{\mathrm{CDCC}}(\vec{r},\vec{R}) = \sum_{i=0}^{i_{\max}} \hat{\phi}_i(\vec{r})\hat{\chi}_i(\hat{K}_i,\vec{R})$$

Test of the two assumptions

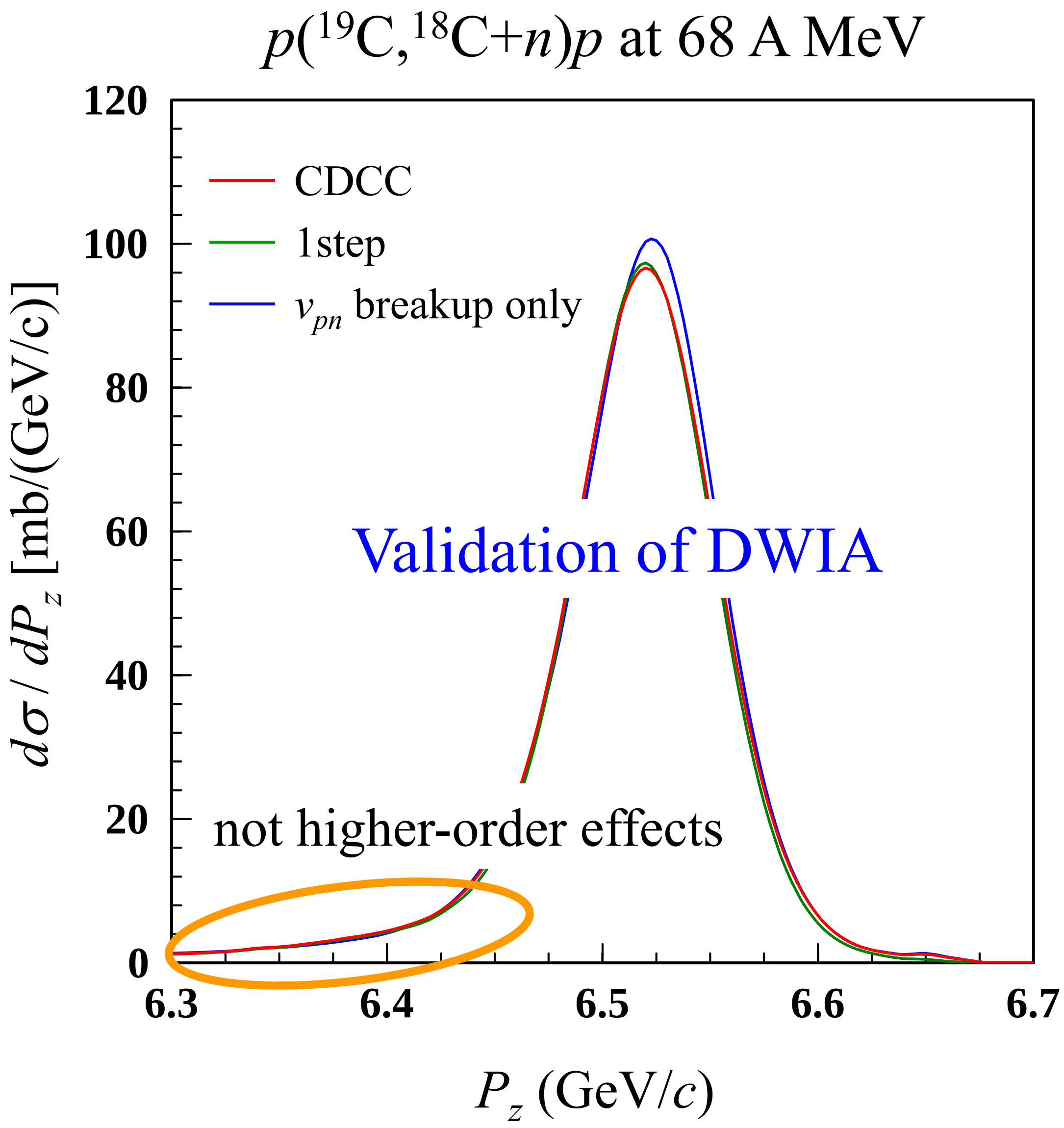

DWIA vs. Faddeev-AGS

R. Crespo *et al.*, PRC**77**, 024601 (2008); PRC**90**, 044606 (2014).

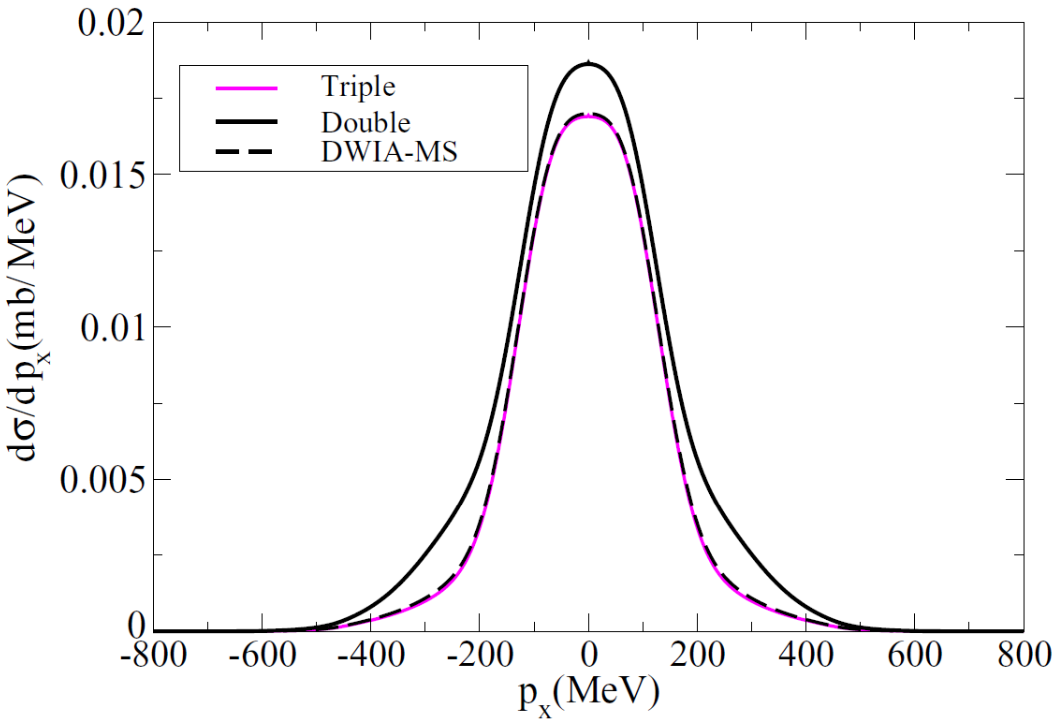

FIG. 8. (Color online) ^{11}B core transverse momentum distribution for the ^{12}C$(p,2p)^{11}$B reaction at 400 MeV/u. The curves represent the observable calculated to second and third orders in the multiple scattering expansion using all the Faddeev-AGS terms and with a truncated series as in the DWIA reaction approach.

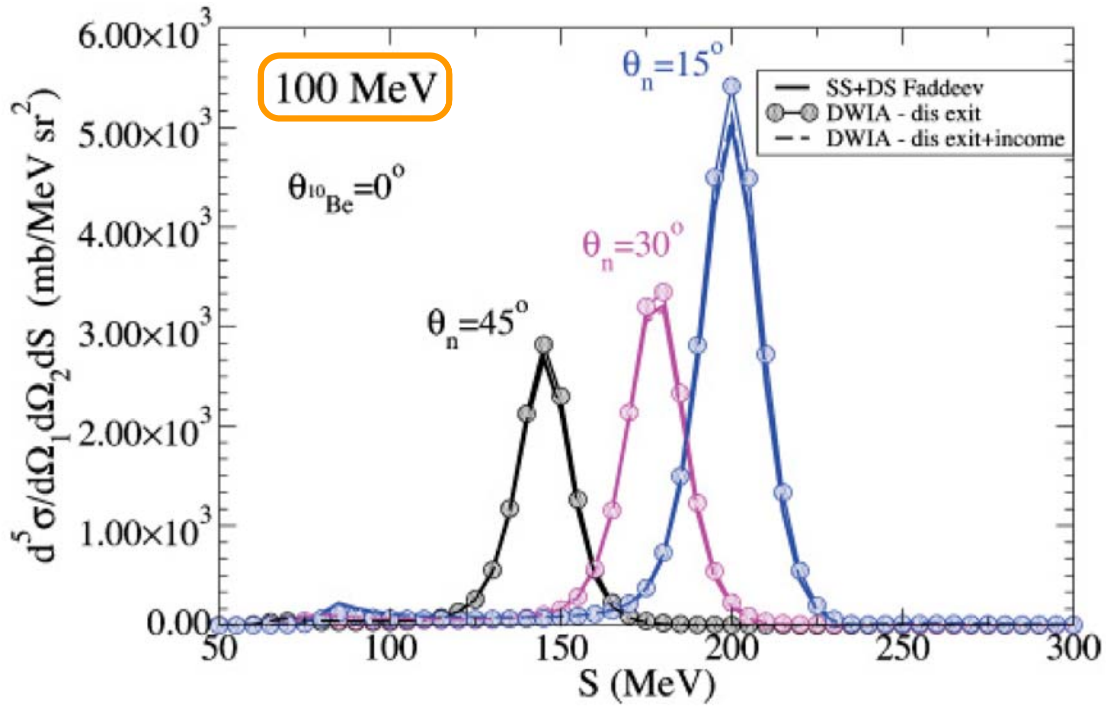

FIG. 15. (Color online) Cross section for the breakup ^{11}Be(p,pn) at 100 MeV.

Eikonal (non-adiabatic) DWIA

A-rest frame

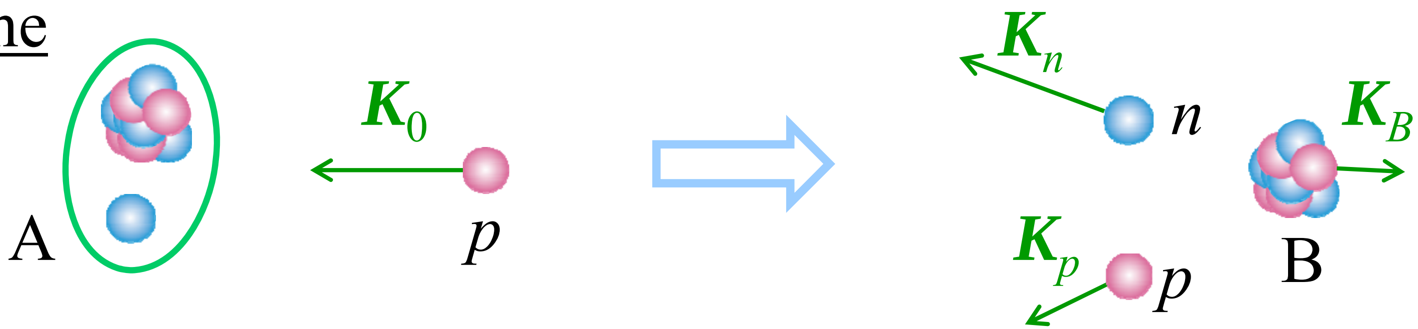

Phase volume

$$\frac{d\sigma}{d\boldsymbol{K}_B d\hat{\boldsymbol{K}}_p} = C_0 \int K_p^2 dK_p d\boldsymbol{K}_n \, \delta\left(\boldsymbol{K}_p + \boldsymbol{K}_n + \boldsymbol{K}_B - \boldsymbol{K}_0\right) \delta\left(E_p + E_n + E_B - E_0\right)$$

$$\times \quad \bar{\sigma}_{NN}\left(\bar{E}_{NN}\right) \left| \int d\boldsymbol{R} \, e^{i\boldsymbol{K}_B \cdot \boldsymbol{R}} F_{K_0 K_p K_n}(b, z) \, \varphi_{n,lj}(\boldsymbol{R}) \right|^2 ,$$

averaged value

"Mom. dist." of nucleon in A

DW factor

$$F_{K_0 K_p K_n}(b, z) \equiv \exp\left[\frac{-i}{\hbar v_p} \int_{-\infty}^{z} U_p(b, z') \, dz'\right] \exp\left[\frac{-i}{\hbar v_n} \int_{-\infty}^{z} U_n(b, z') \, dz'\right]$$

$$\times \exp\left[\frac{-i}{\hbar v_0} \int_{z}^{\infty} U_0(b, z') \, dz'\right]$$

cf. T. Aumann, Bertulani, Ryckebusch, PRC**88**, 064610 (2013).

Eikonal calculation for elastic scattering

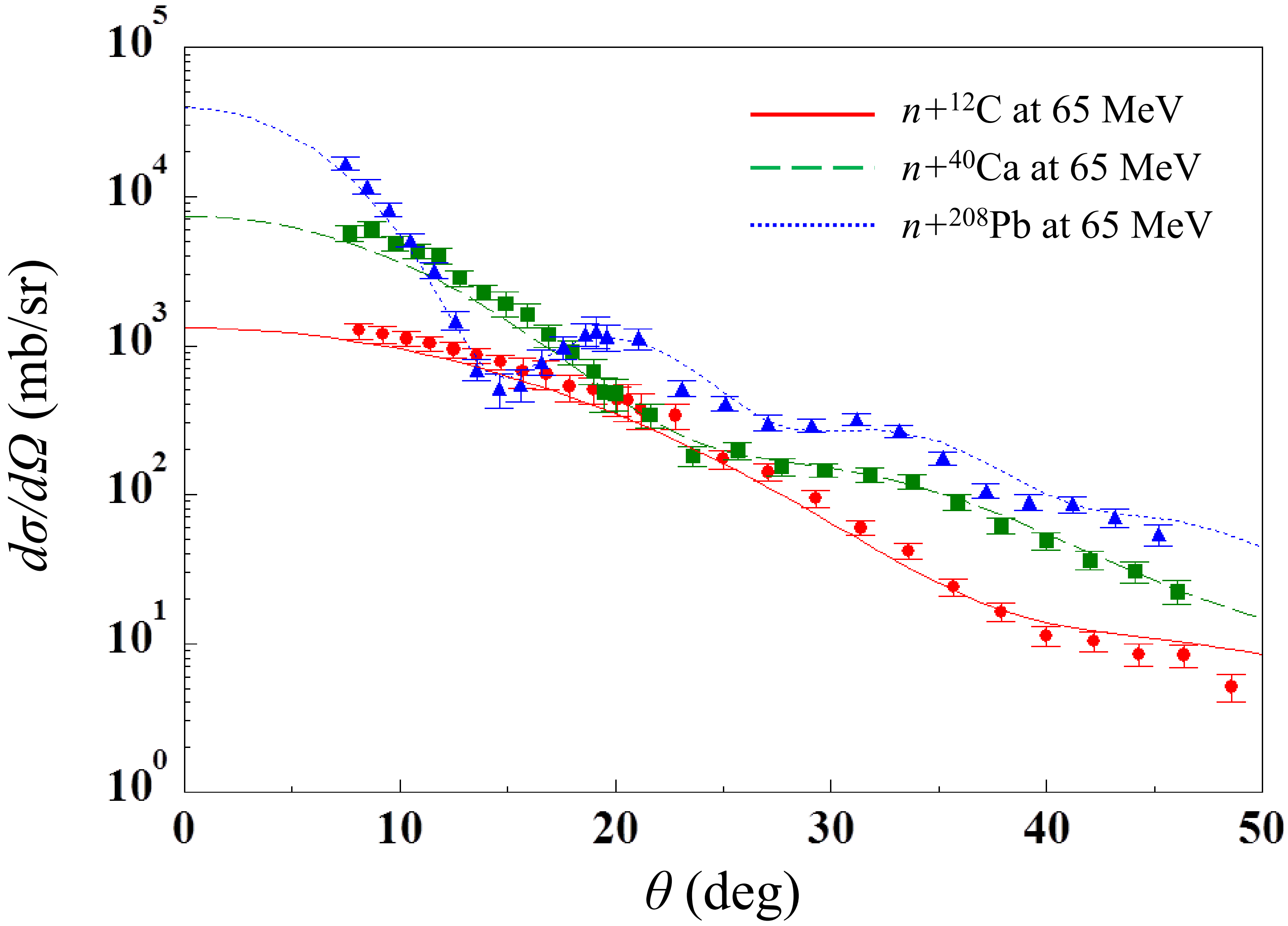

KO, "Introduction to quantum scattering theory", in preparation.

Validation of the eikonal DWIA

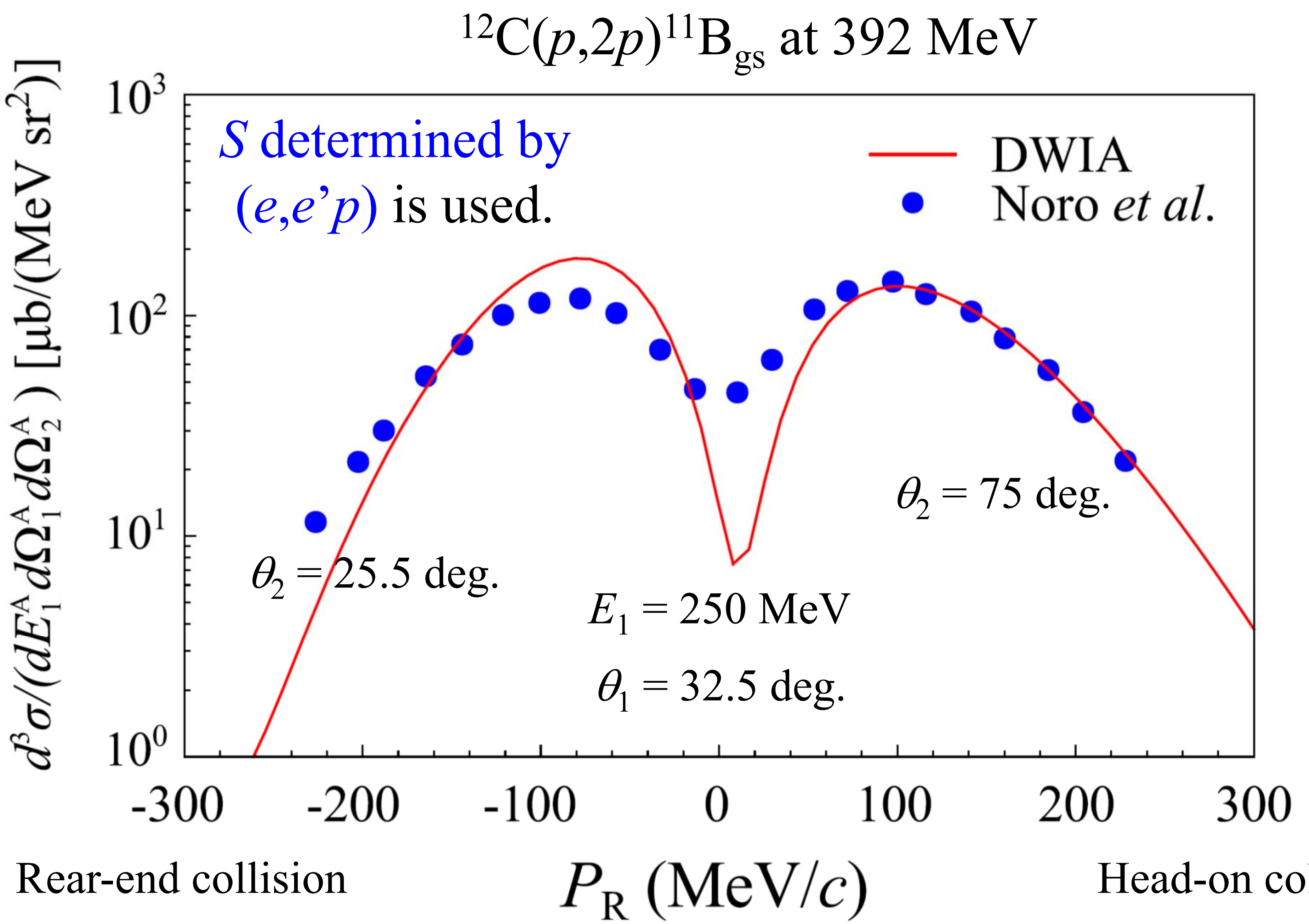

Rear-end collision

Head-on collision

Exp. data: T. Noro, private communication (2014).

Theory vs. exp. data for (e,e'p)

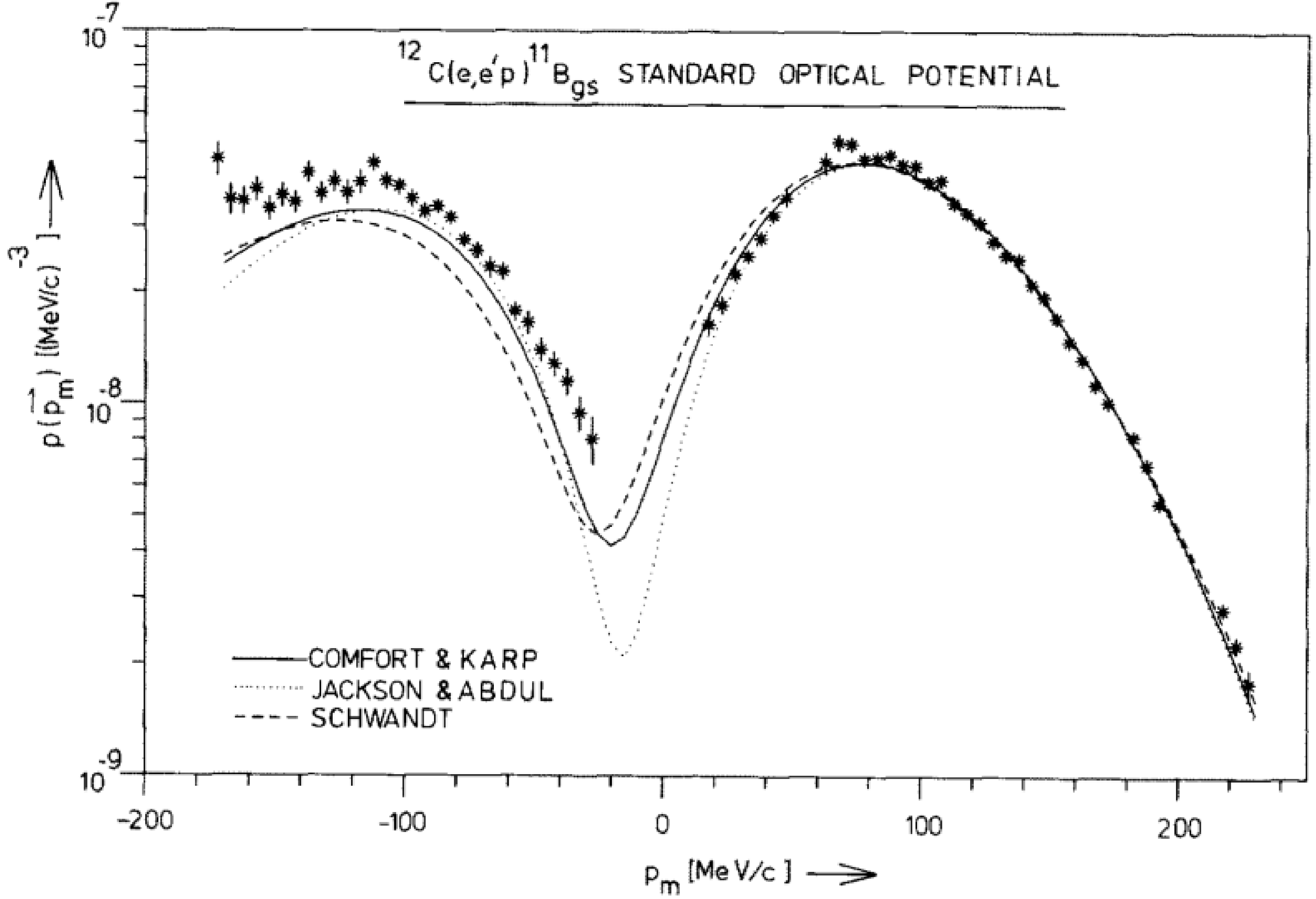

G. V. D. Steenhoven *et al*., NPA **480**, 547 (1988)

Opt. Pot. Dep.

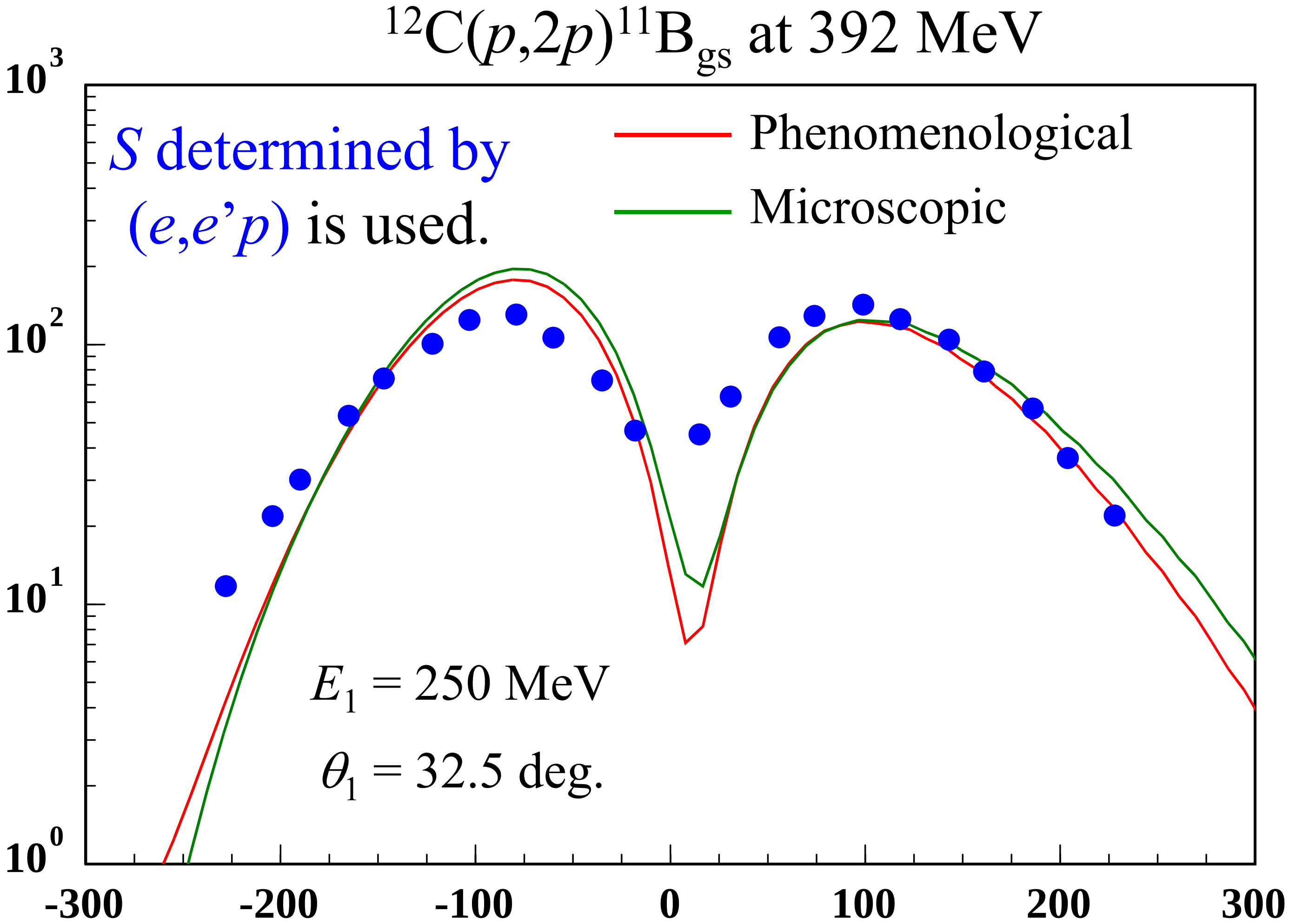

Exp. data: T. Noro, private communication (2014).

S factors from (d,^{3}He): “now” and past

G. J. Kramer, Blok, Lapikas, NPA **679**, 267 (2001).

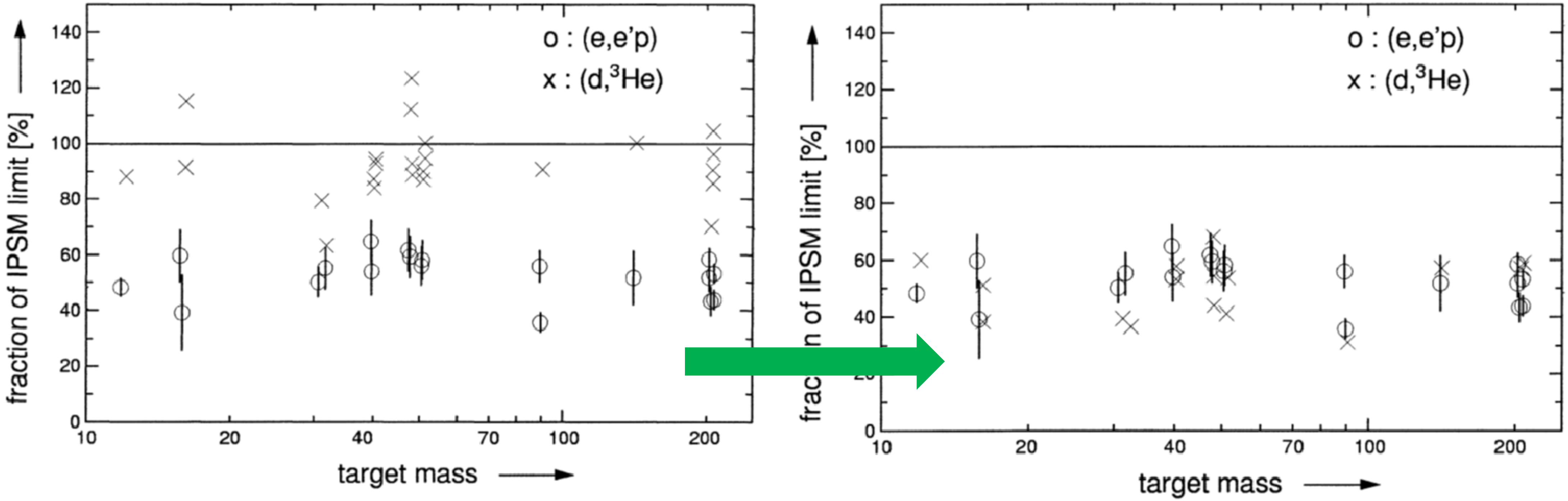

In this article it has been shown that spectroscopic factors obtained from (e,e′p) and (d,^{3}He) experiments are mutually consistent, provided that in the DWBA calculations for the analysis of the (d,^{3}He) data nonlocality and finite-range corrections are included together with the BSWF obtained from (e,e′p) experiments. It was also shown that the (e,e′p) reaction is sensitive to the whole BSWF, whereas the (d,^{3}He) reaction is only sensitive to the exponential tail of the BSWF. This tail is very sensitive to the assumed shape of the potential well used to generate the BSWF.

MD calculation with Eikonal DWIA

A-rest frame

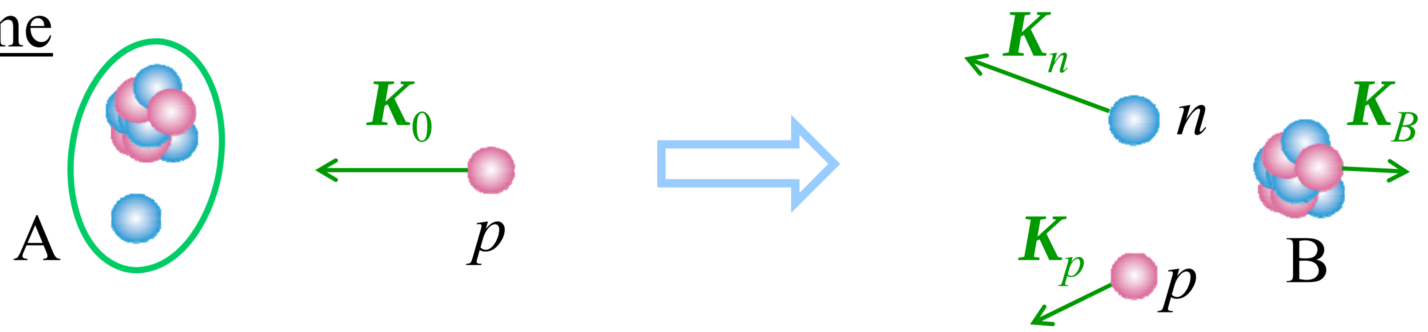

MD of B

Phase volume

$$\frac{d\sigma}{d\boldsymbol{K}_B} = C_0 \int d\boldsymbol{K}_p d\boldsymbol{K}_n \, \delta\left(\boldsymbol{K}_p + \boldsymbol{K}_n + \boldsymbol{K}_B - \boldsymbol{K}_0\right) \delta\left(E_p + E_n + E_B - E_0\right)$$

$$\times \bar{\sigma}_{NN}\left(\bar{E}_{NN}\right) \left| \int d\boldsymbol{R} \, e^{i\boldsymbol{K}_B \cdot \boldsymbol{R}} F_{K_0 K_p K_n}(b, z) \, \varphi_{n,lj}(\boldsymbol{R}) \right|^2$$

DW factor

$\equiv \mathfrak{F}_{\boldsymbol{K}_B}$

PWIA (for analysis)

$$\frac{d\sigma^{\rm PW}}{d\boldsymbol{K}_B} = \bar{\rho}\left(\boldsymbol{K}_B\right) C_0 \bar{\sigma}_{NN}\left(\bar{E}_{NN}\right) \left| \int d\boldsymbol{R} \, e^{i\boldsymbol{K}_B \cdot \boldsymbol{R}} \varphi_{n,lj}(\boldsymbol{R}) \right|^2,$$

$$\bar{\rho}\left(\boldsymbol{K}_B\right) \equiv \frac{\pi m}{\hbar^2} \sqrt{\left(\boldsymbol{K}_0 + \boldsymbol{K}_B\right)^2 - \frac{2A}{A-1} K_B^2 - \frac{4m}{\hbar^2} S_N}.$$

PMD of ^{13}O for ^{14}O(p,pn)^{13}O at 100 A MeV

S_n = 23.2 MeV (0p3/2), S factor = 1

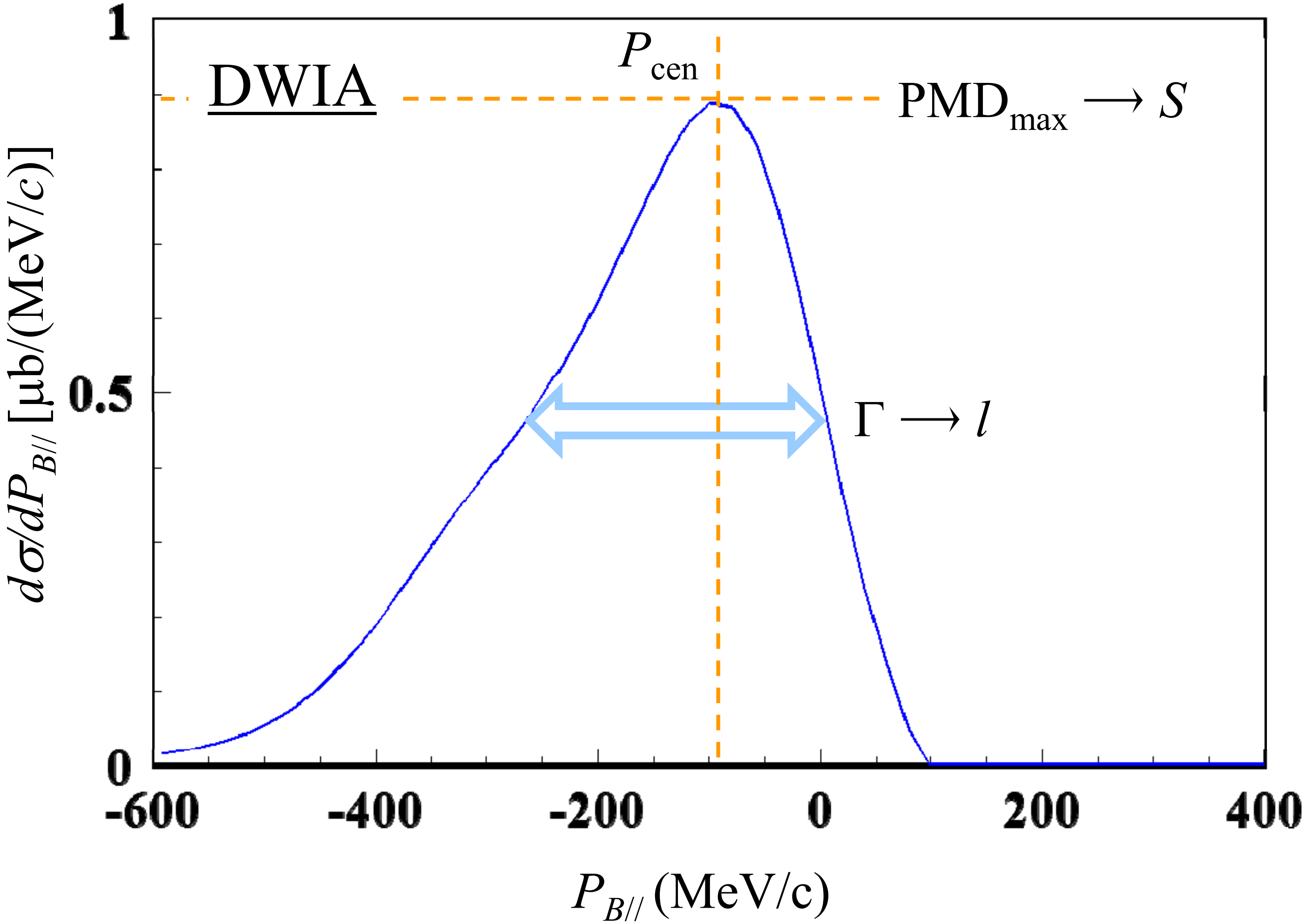

A-rest frame

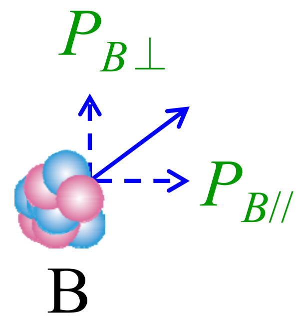

Can we interpret the PMD as the nucleon MD inside ^{14}O?

Phase volume (PV) effect on the PMD

S_n = 23.2 MeV (0p3/2), S factor = 1

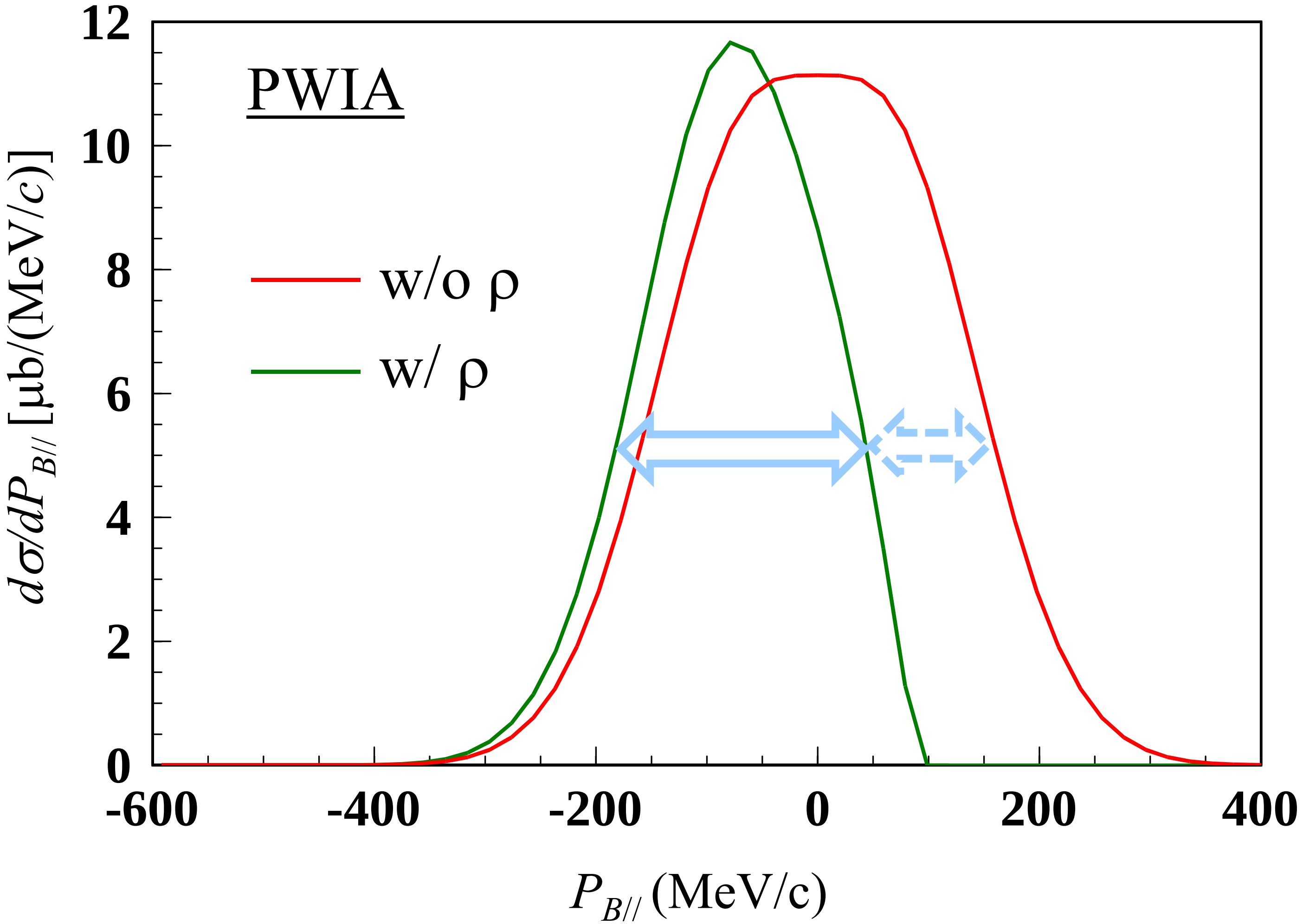

A-rest frame

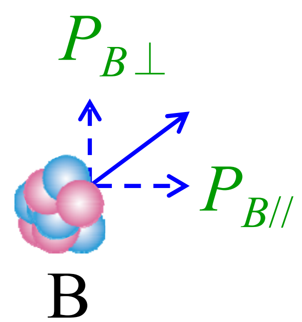

- The PV effect gives a cut on the high-mom side resulting in a reduction of Γ.
- The PMD height changes little and the integrated PMD decreases significantly.

PV effect on the MD

$^{14}O(p,pn)^{13}O$ at 70 A MeV

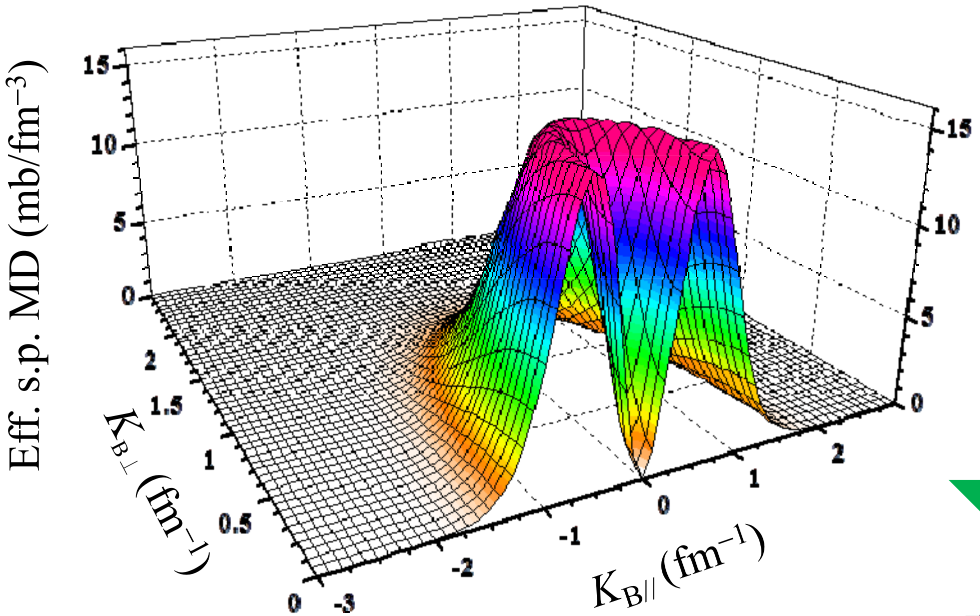

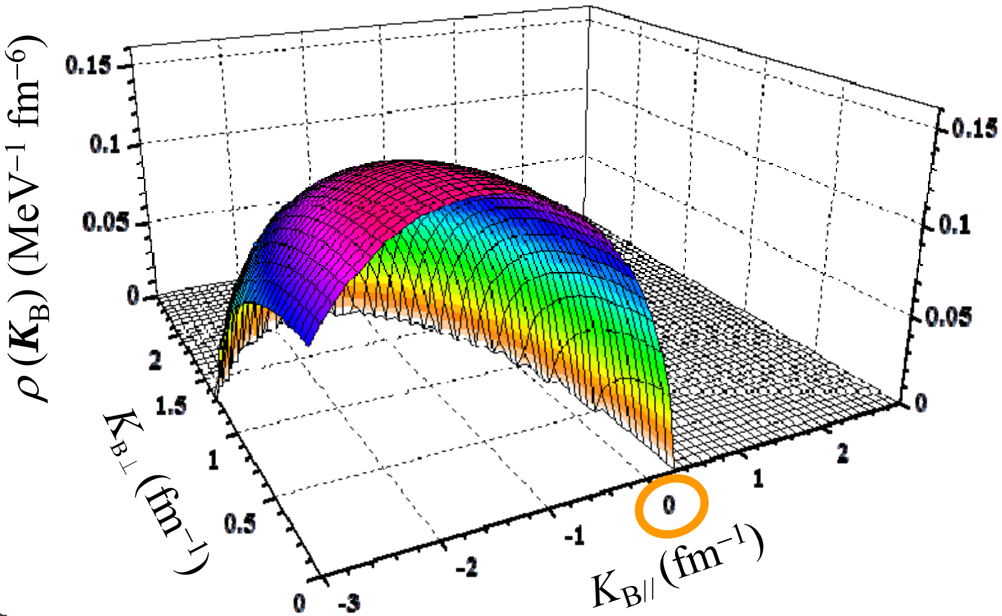

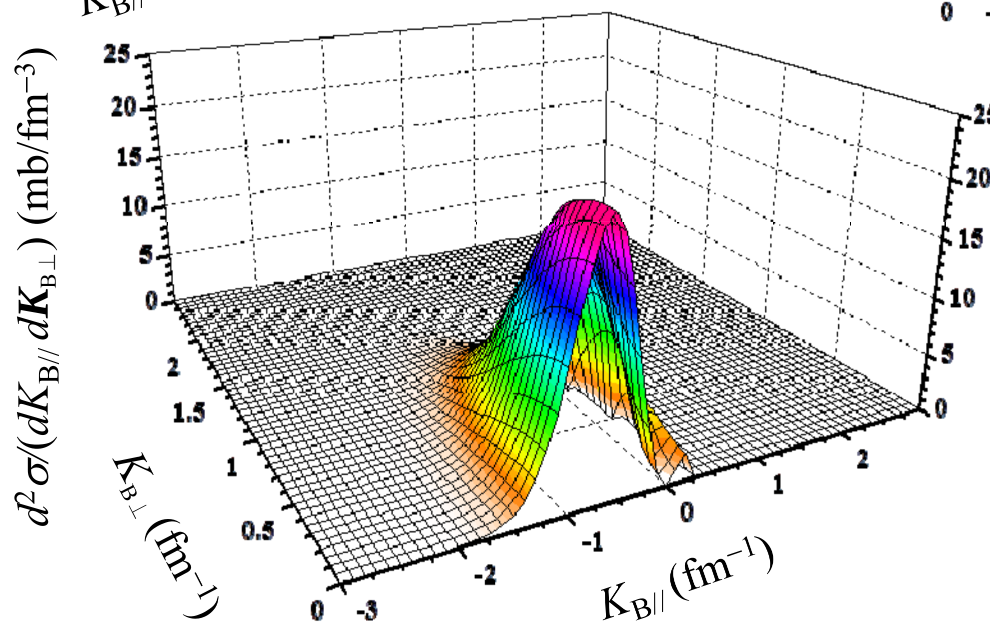

Phase volume effect

A-rest frame

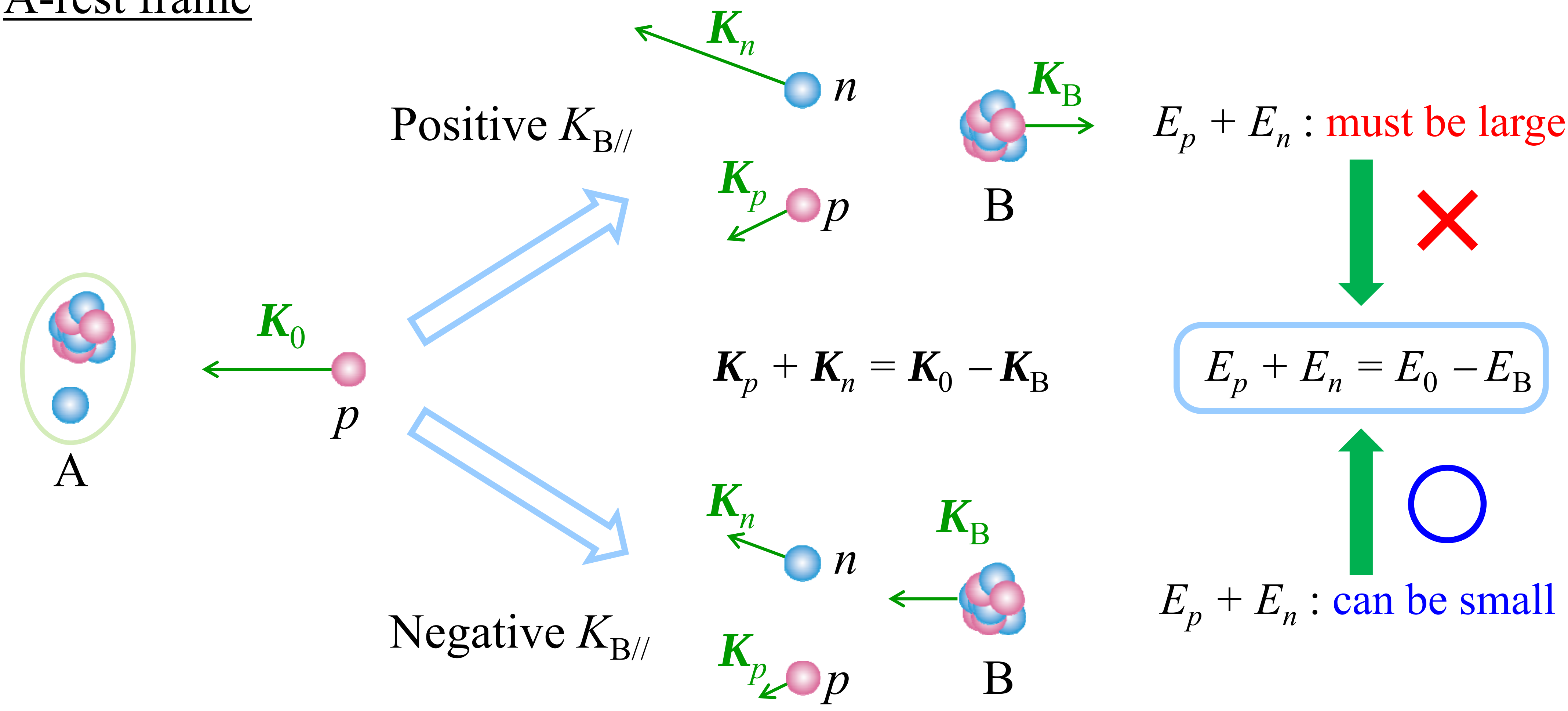

$$\bar{\rho}\left(\boldsymbol{K}_B\right) \equiv \frac{\pi m}{\hbar^2}\sqrt{\left(\boldsymbol{K}_0 + \boldsymbol{K}_B\right)^2 - \frac{2A}{A-1}K_B^2 - \frac{4m}{\hbar^2}S_N}.$$

Phase volume (PV) effect on the PMD

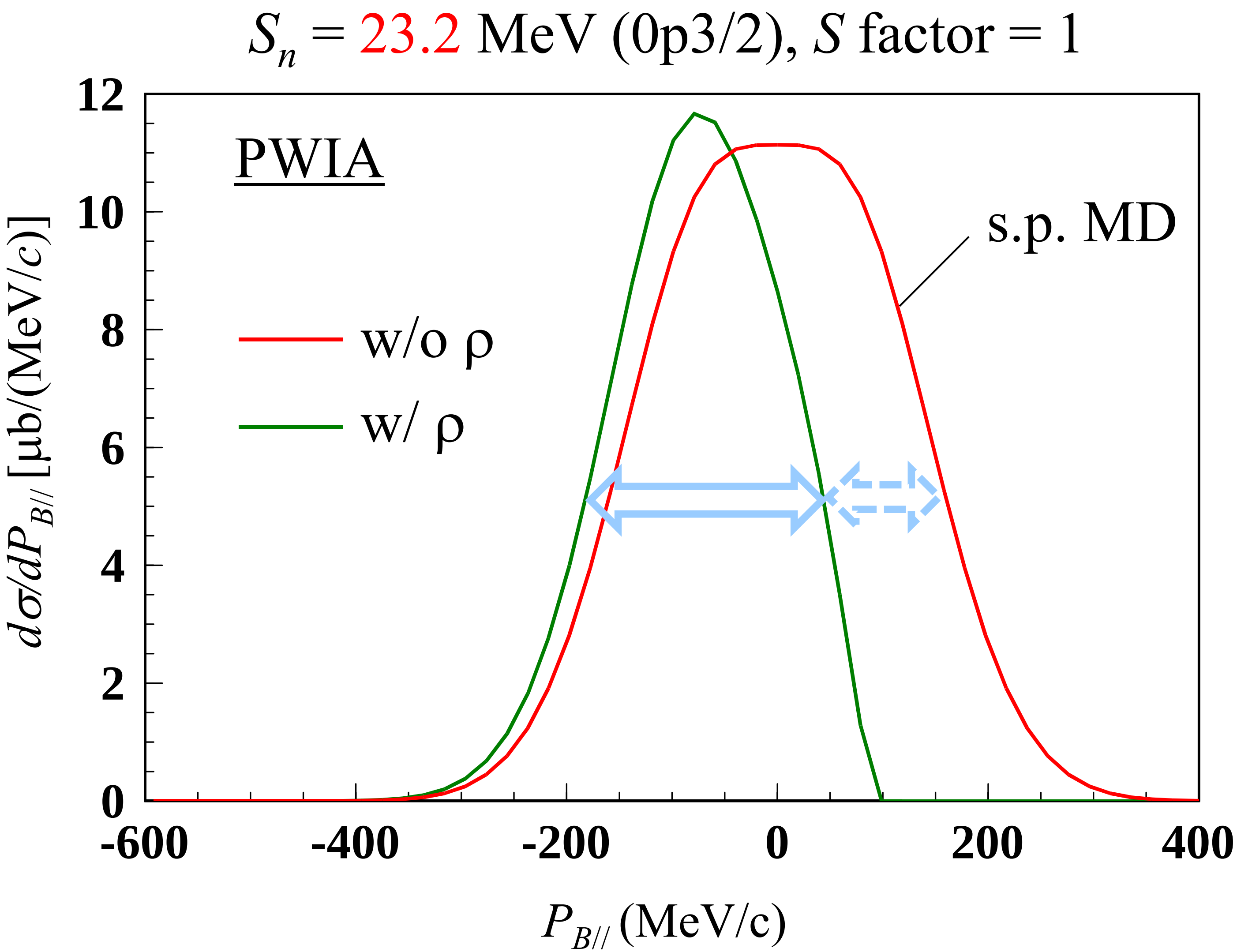

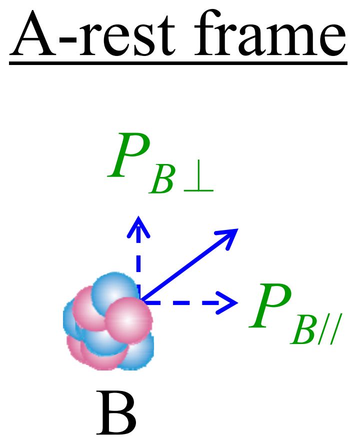

- The PV effect gives a cut on the high-mom side resulting in a reduction of Γ.
- The PMD height changes little and the integrated PMD decreases significantly.

Distortion effect on the PMD

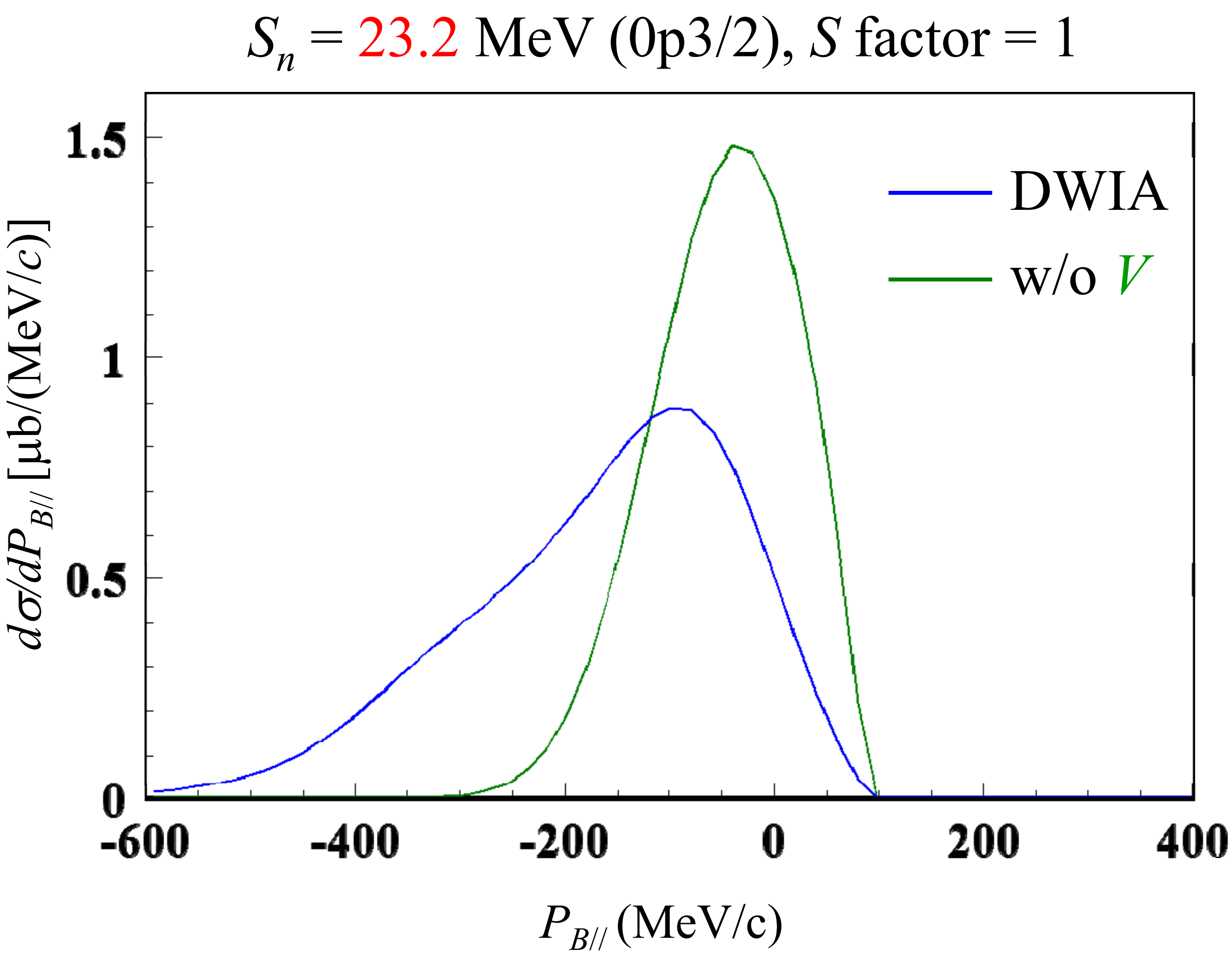

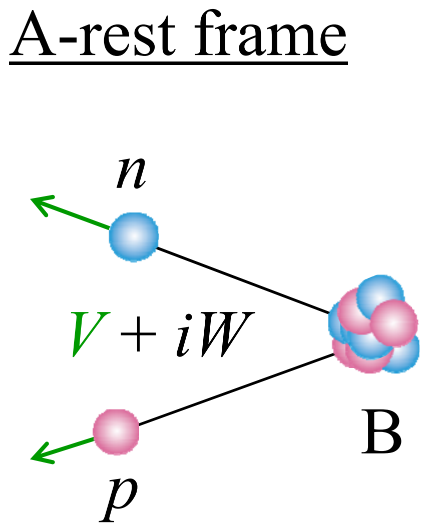

- Attractive (real) potential of B gives the low-momentum tail.
- The PMD height changes significantly and the integrated PMD changes little.

Distortion effect on the MD

$^{14}O(p,pn)^{13}N$ at 70 A MeV

PWIA

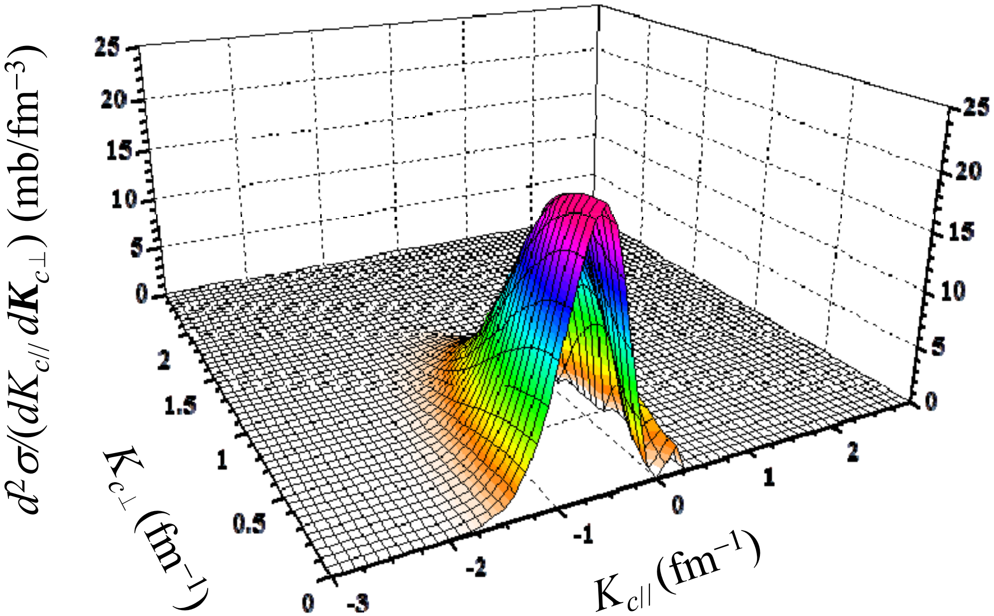

DWIA

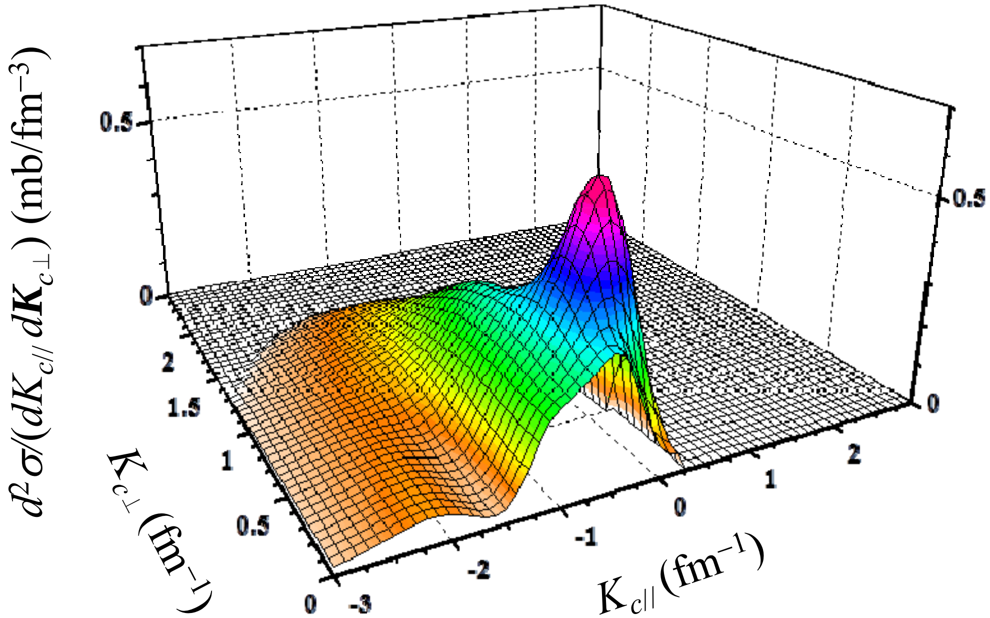

- Distortion generates the low momentum tail in the PMD and widens the transverse MD.
- This is due to the asymmetry in the kinematics of the 3-body system.

Distortion effect on the TMD

S_n = 23.2 MeV (0p3/2), S factor = 1

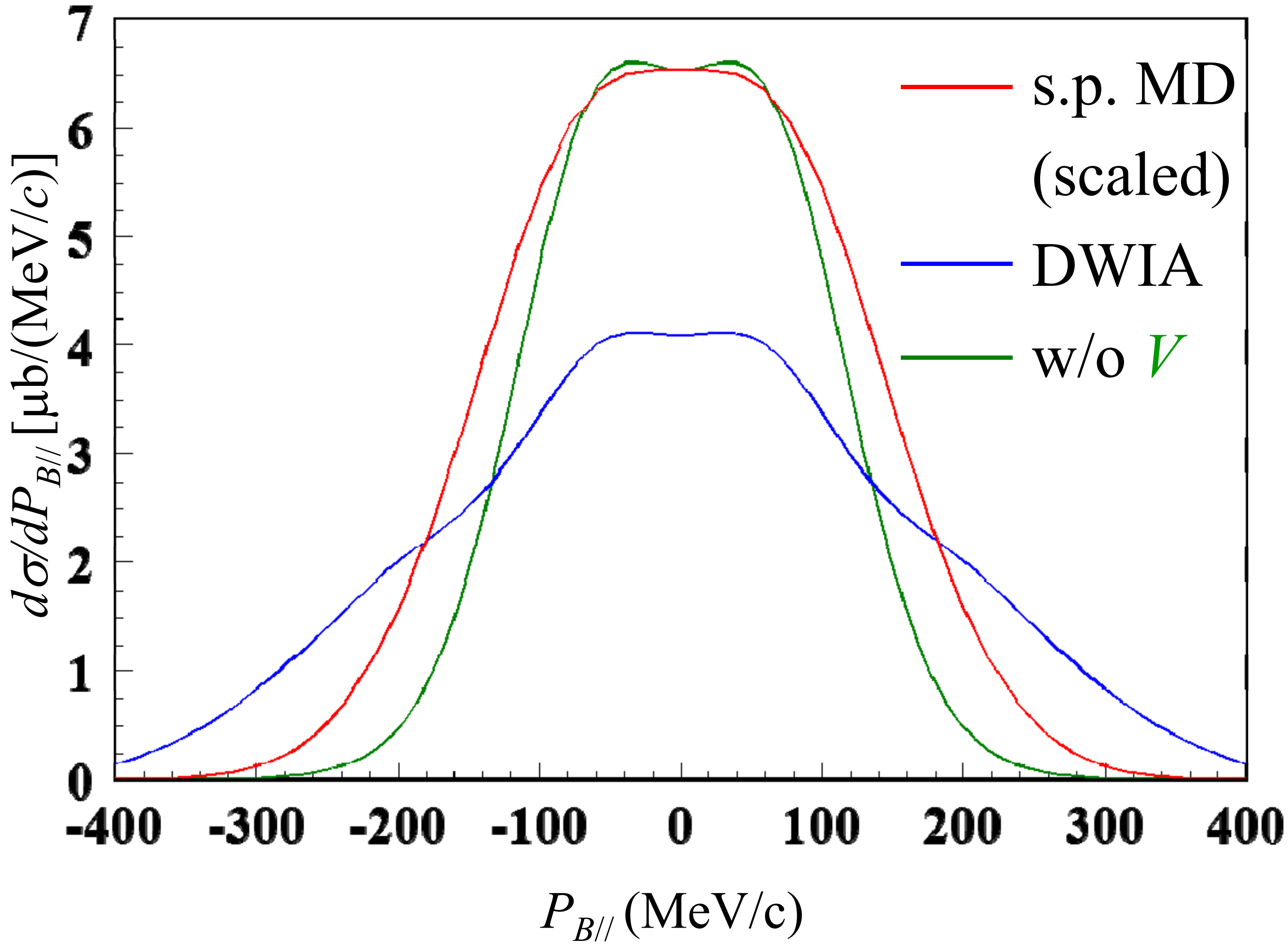

A-rest frame

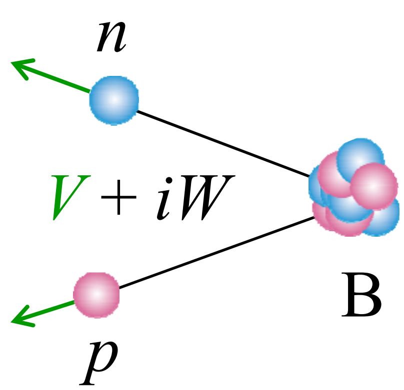

- Distortion widens the width and even changes the shape.

Asymmetry in the PMD of $^{14}O(p,pn)^{13}O$

KO, Yoshida, Minomo, PRC **92**, 034616 (2015).

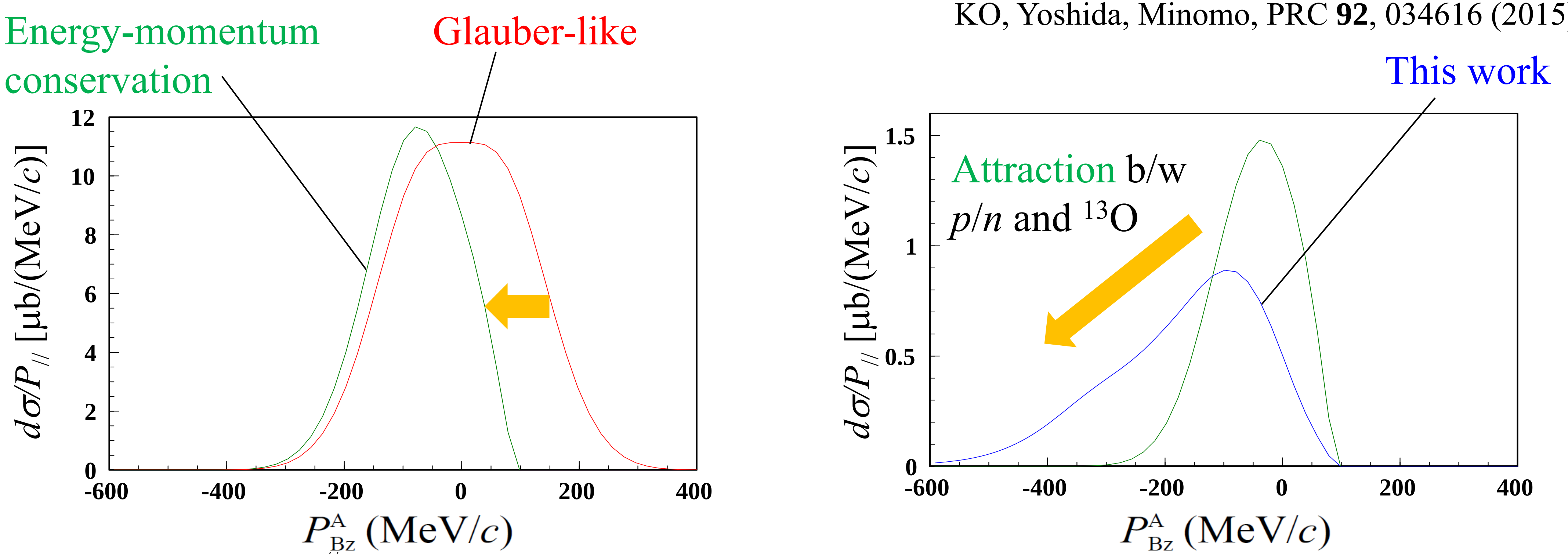

- ✓ The Glauber-like calc. overshoots both the integrated X-sec. and the peak height, possibly resulting in overestimation of the missing correlation.
- ✓ PV and distortion effects exist also in nucleon removal processes with a nucleus target, and will affect the reduction factor.
- ✓ Studies on the reduction factor with a proton target are going on (collaboration with Uesaka-san's group).

Summary (1/2)

- Some reaction models for describing EB and KO reactions are reviewed.
  - CDCC/Glauber is designed with assuming small ω-q, i.e., breakup of a weakly-bound nucleus.
  - DWIA is suitable for describing large ω-q processes. (Use of a proton target will make the reaction process the simplest.)
  - The Glauber model (AD approx.) becomes questionable when ω-q is large, which results in failure in reproducing the asymmetric shape of the PMD.
  - DWIA is equivalent to CDCC when the coupling to the breakup states of the c+n nucleus is negligible and the breakup is caused by only the n-target int.; this is the case even for ^{19}C(p,pn)^{18}C at 68 A MeV.
  - DWIA is more flexible than CDCC because it can include E-dep. complex c-n potential and large values of their relative ang. mom. l easily.

Summary (2/2)

- $(p,2p)/(p,pn)$ is an established method for clarifying s.p. properties of nuclei.
  - no stripping process
  - intuitive picture of the reaction process
  - observation of nuclear interior (not only the tail region)

- We have clarified that the asymmetric shape of the PMD comes from the asymmetry in the kinematics:
  - the phase volume effect that cuts the high-momentum side of the PMD, with reducing its integrated value, and
  - the distortion effect that generates the tail on the low-mom. side, decreasing the peak height of the PMD.

  If these two are properly taken into account, the PMD/TMD will be useful to extract s.p. information.

Future perspective

- Spectroscopic studies with (*p*,*pN*)
  - A computer code PIKOE will be available soon. [O & Yoshida (RCNP)]
  - A microscopic *N*-*A* opt. pot. will be given by a code SFOLC.
  - Systematics of the reduction factor [Kawase, Obertelli, …]
- Nuclear correlation studies
  - (*p*,*p*α) / (*p*,*pd*) reactions as a probe of α / *d* correlation [Beaumel, Zaihong, Yoshida (Niigata)]
  - (*p*,*pNN'*) as a probe of 2*N* correlations
- (*p*,*pN*) as a tool to populate a particle-unbound state
  - *nn* correlation in the ground state of a Borromean nucleus [Kikuchi]
  - Decay of the reaction residue in continuum [Watanabe/JAEA]
- Studies on 3NF effects via (*p*,*pN*) [Minomo]
- DWIA for high-energy (*p*,*d*) reactions for tensor studies [Ong, Pang]